ChemCatBio
Chemical Catalysis for Bioenergy

Advancing Catalytic Fast Pyrolysis through Integrated Experimentation and Multi-Scale Computational Modeling

Michael Griffin, Brennan Pecha, Bruce Adkins

January 13, 2021

U.S. DEPARTMENT OF ENERGY | Office of ENERGY EFFICIENCY & RENEWABLE ENERGY
BIOENERGY TECHNOLOGIES OFFICE

Catalytic Fast Pyrolysis (CFP) Overview

Biomass Harvesting → Feedstock Pre-Processing → Fast Pyrolysis → Vapor Phase Catalytic Upgrading → Hydrotreating and Fractionation

CFP is an adaptable pathway for the conversion of woody biomass and waste carbon sources into fuel blendstocks and chemical co-products

Ruddy, D. et al. *Green Chem*., **2014**, 16, 454
Langholtz, M. H., et al. 2016 Billion Ton Report, US DOE, ORNL-TM2016-160

Approach to Catalytic Fast Pyrolysis

In-Situ CFP

Ex-Situ CFP

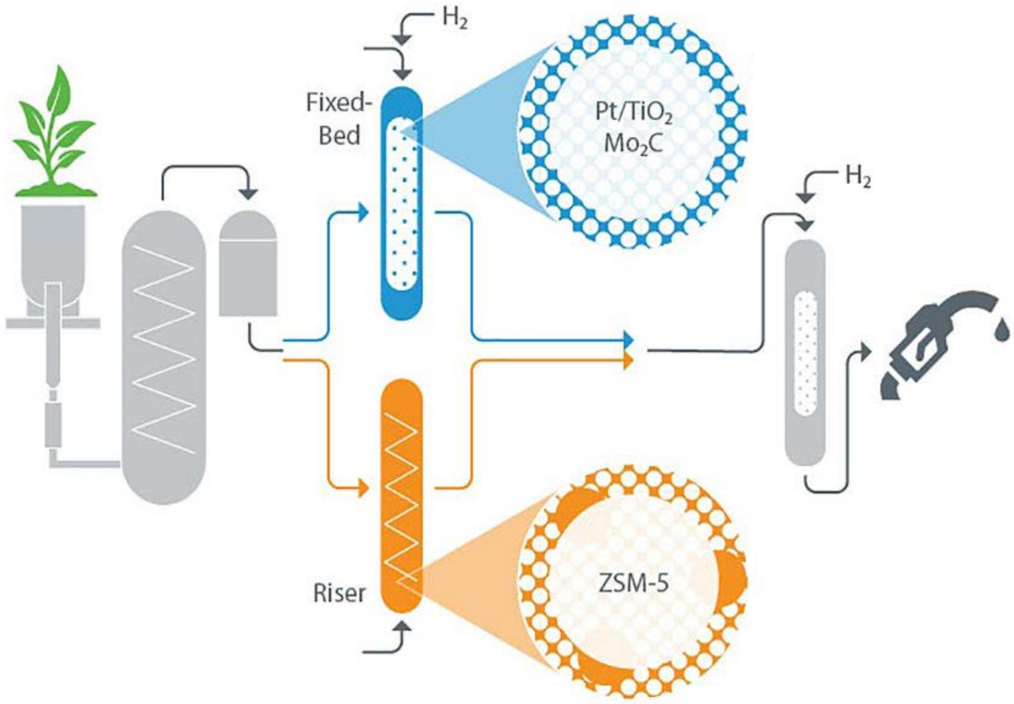

Technical approaches include different catalysts and reactor configurations

Fluidized Bed Zeolite CFP

Pilot and demonstration scale data demonstrate the technical feasibility of the approach

Challenge: Rapid coking lowers yields, necessitates frequent regeneration, and drives up fuel costs

Fixed Bed Hydrodeoxygenation

Fundamental research highlights opportunities for enhanced performance

Gap: Lack of realistic reaction testing data increases risk and uncertainty

Integrated Reaction Testing With Biomass

Feedstock

Debarked Loblolly Pine and Forest Residues

Idaho National Lab

Catalyst

0.5-2.0 wt% Pt/TiO_2 on Technical Supports

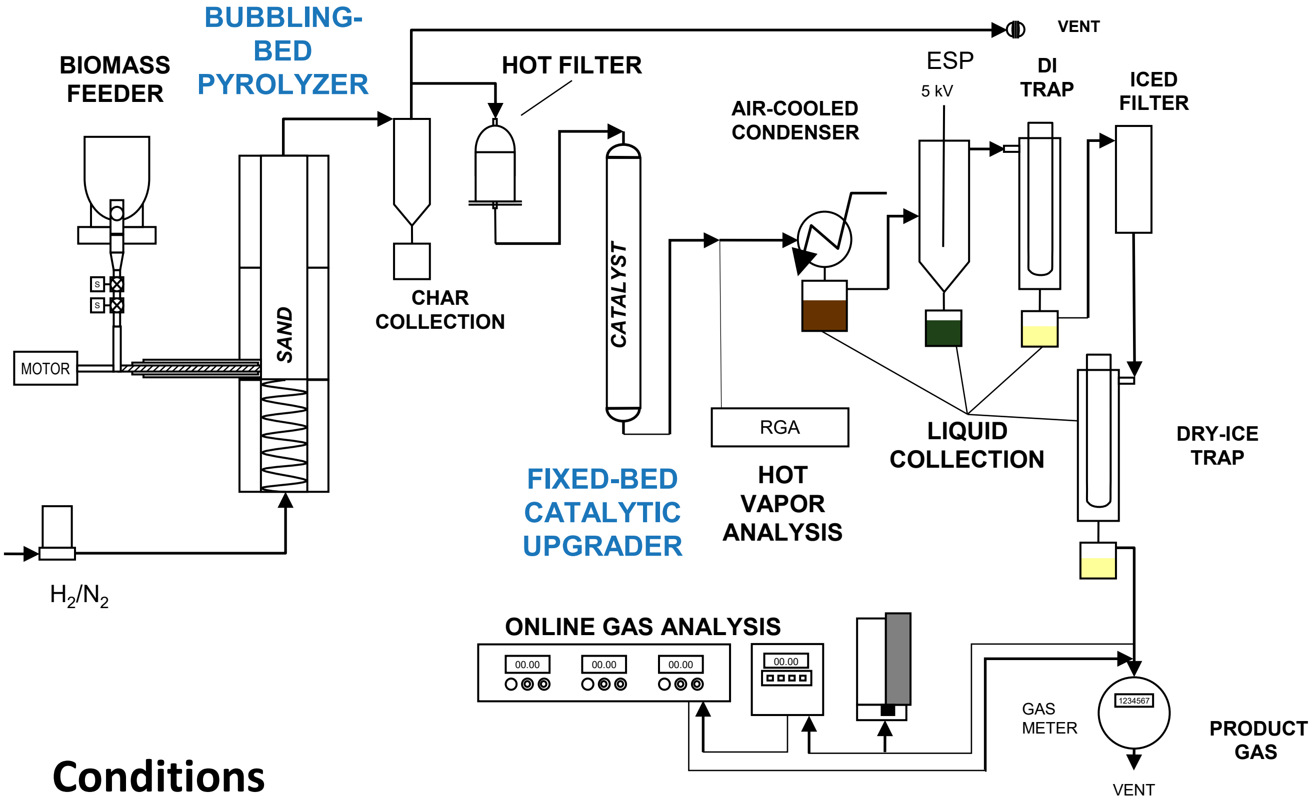

Conditions

Pyrolysis Temperature: 500 °C
Upgrading Temperature: 435-450 °C
Catalyst Mass: 100 g

WHSV: 1.4 g biomass/gcat*h
Biomass:Catalyst Ratio: 3-13.2
Hydrogen Concentration: 83%

> 10 L of CFP-oil produced over 100+ reaction cycles

Reaction Testing Highlights Improved Performance

Pt/TiO_2 exhibited **improved carbon yields** at similar oxygen content compared to ZSM-5

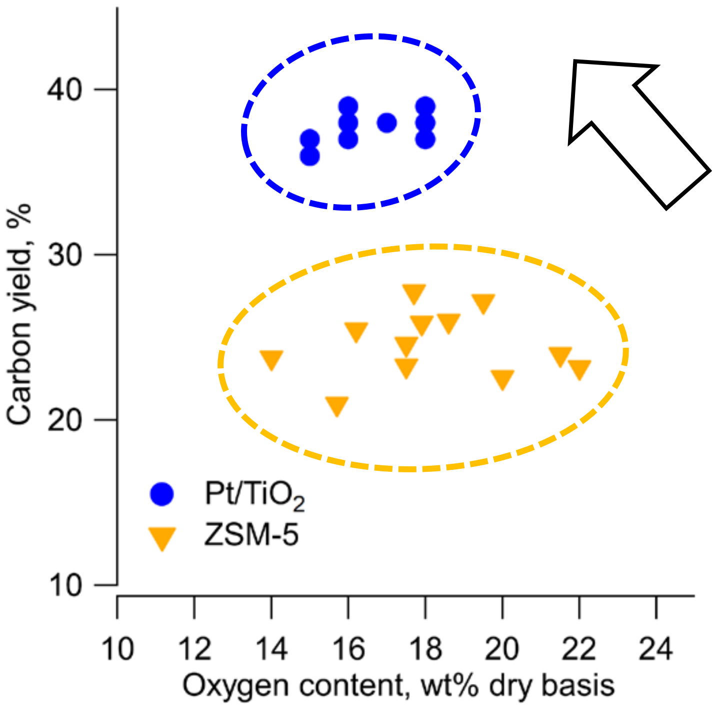

V. Paasikallio, et al. *Energy Technol* 5, **2017,** 94
V. Paasikallio, et al. *Green Chem* 16, **2014,** 3549

Pt/TiO_2 exhibited **stable performance** over 100+ reaction/regeneration cycles

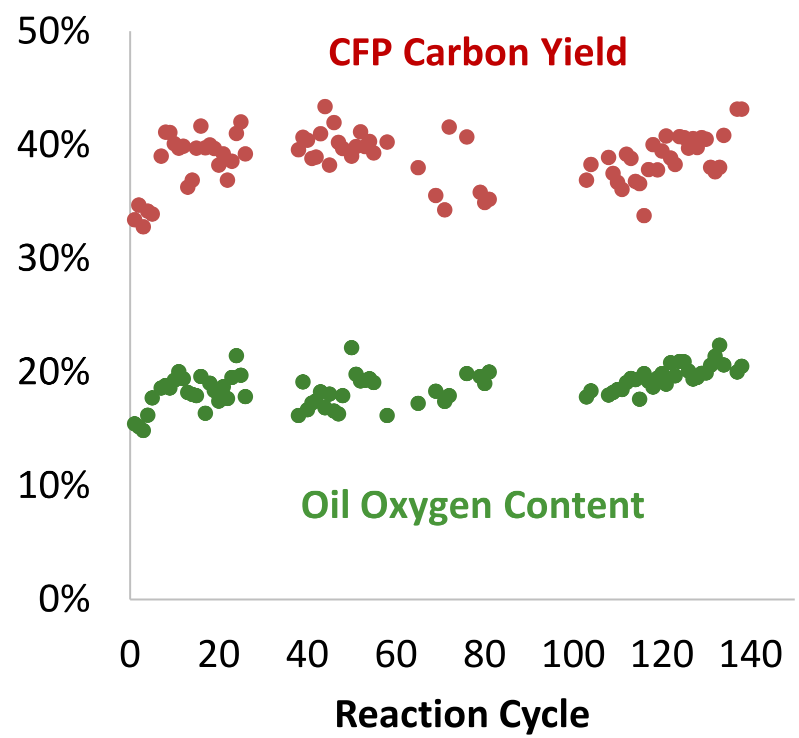

Griffin, M. et al., Energy Environ Sci, **2018,** 2904
K. Iisa, et al. *Energy Fuels* 30, **2016,** 2144
K. Iisa, et al. *Top Catal* 59, **2016,** 94

Stable Single Stage Hydrotreating

The Pt/TiO_2 CFP-oil was hydrotreated using a **single stage** system for 80+ hours without fouling or plugging

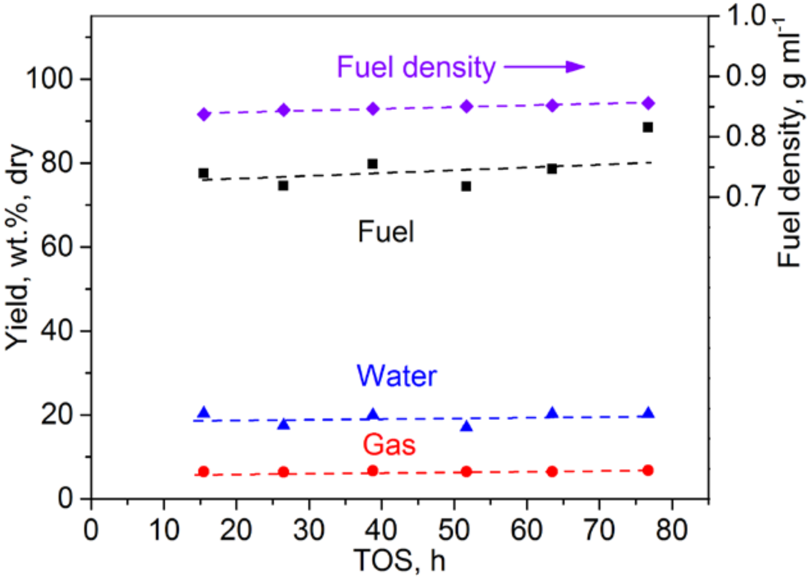

Carbon yield %	H/C mol/mol	O wt.% dry	Density g ml^{-1}
89	1.71	0.19	0.851

NiMo Sulfide, LHSV: 0.2-0.3, 13 MPa

Pacific Northwest
NATIONAL LABORATORY

Fractionation indicates high selectivity to the distillate range

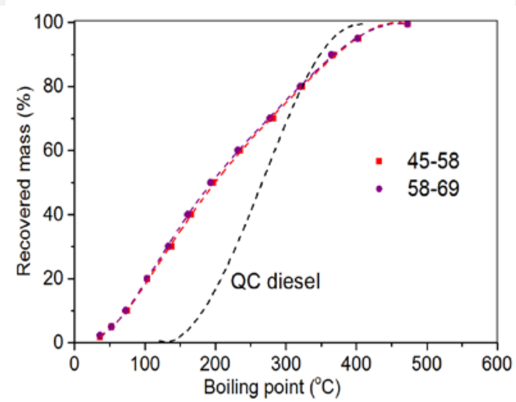

45 wt% in gasoline range

39 wt% in diesel range

Fuel testing reveals need for continued R&D

	Measured	Target
Gasoline AKI	65	85
Diesel DCN	24	40

CFP provide opportunity to improve fuel quality by controlling hydrogenation and promoting ring opening reactions

Griffin, M. et al., Energy Environ. Sci., 2018, 11, 2904

Technoeconomic and Lifecycle Analysis

Conceptual process models indicate a minimum fuel selling price of $3.80, with an opportunity for further reduction through refinery integration and the generation of chemical co-products

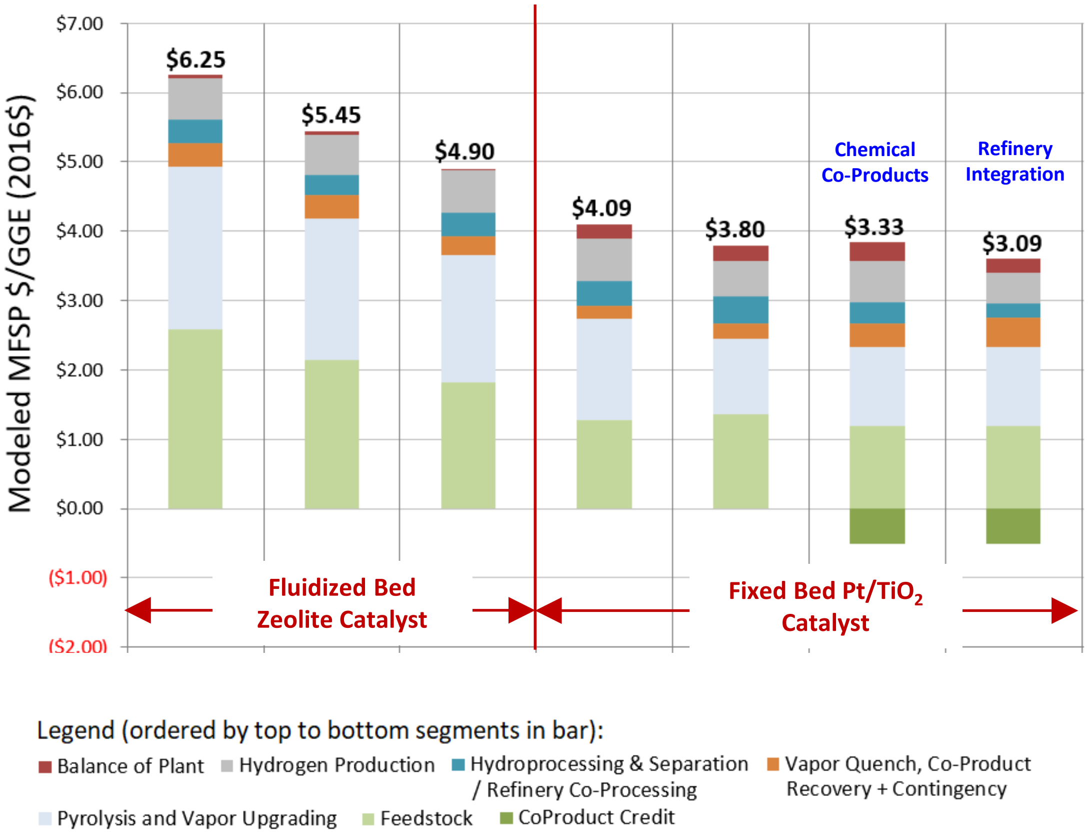

Overall Process Carbon Yield:

36% for Pt/TiO_2

≤ 22% for ZSM-5

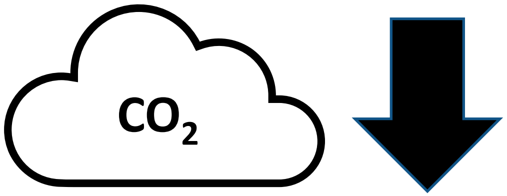

> 50%

Considerable reduction in carbon intensity

Reference: https://www.nrel.gov/docs/fy20osti/76269.pdf; **SOT:** State of Technology; **MFSP:** Minimum Fuel Selling Price

Summary and Research Needs

Integrated reaction testing confirmed potential for improved performance from fixed bed hydrodeoxygenation and motivates investigation of process scale up

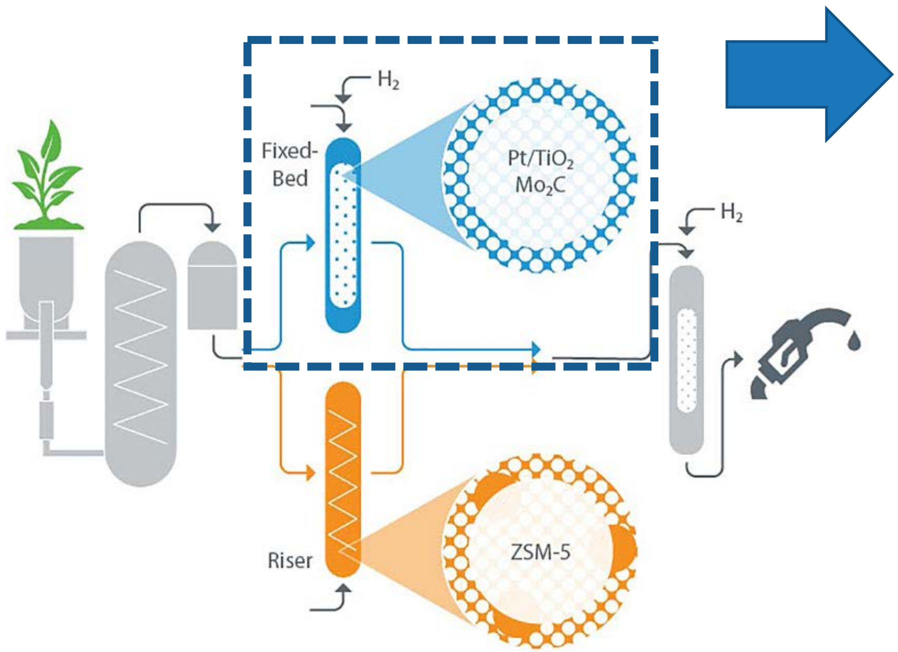

- **High Yields** ✓
- **Improved Economics** ✓
- **Low Emissions** ✓
- **Process Stability** ✓
- **Scalability** ?

Leverage partnerships to perform particle and reactor scale computational modeling to directly address open questions about reaction kinetics and process scale-up

ChemCatBio
Chemical Catalysis for Bioenergy

Teasing out fundamental information from bench top packed bed reactor experiments with multiscale modeling

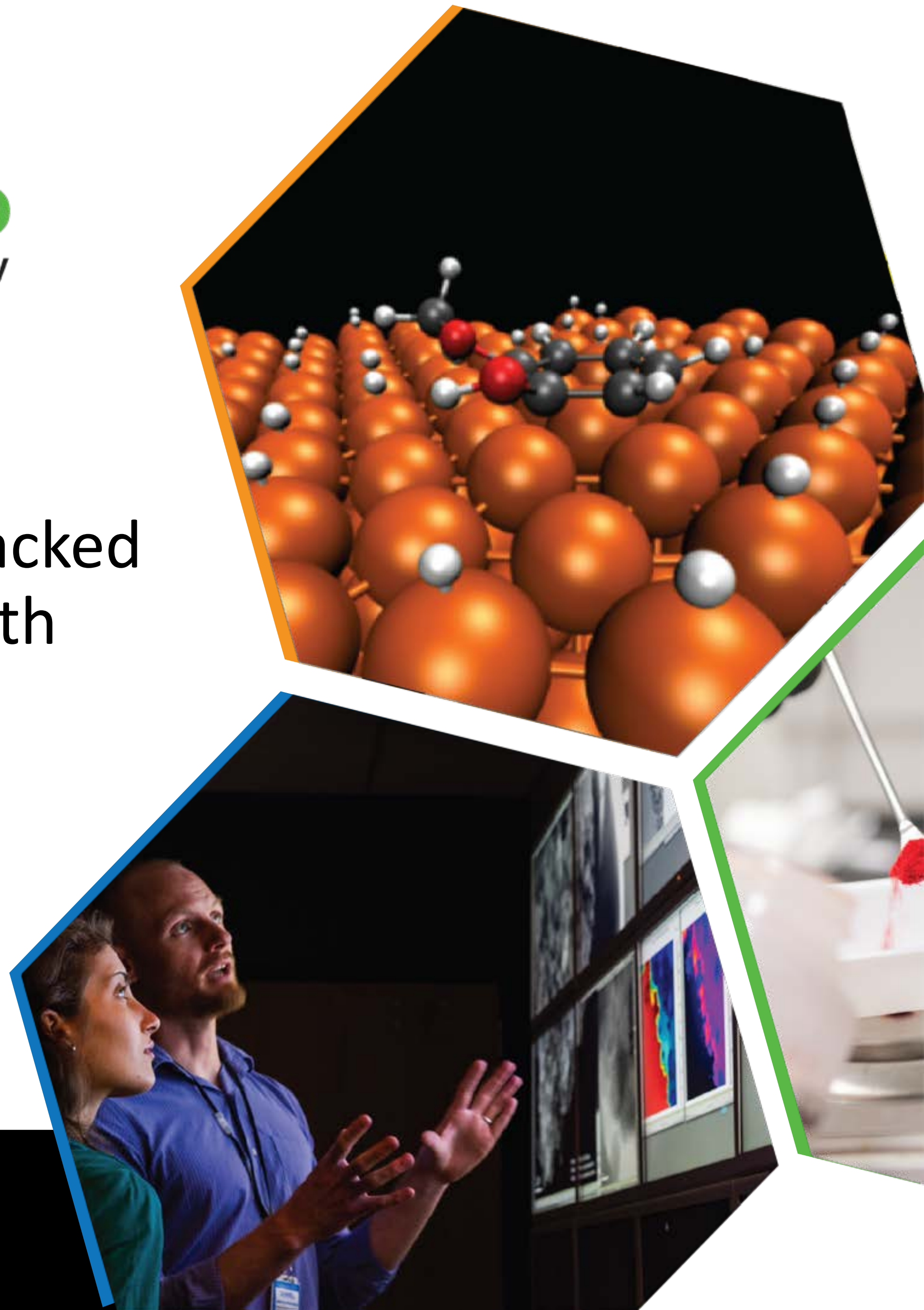

U.S. DEPARTMENT OF ENERGY | *Office of* ENERGY EFFICIENCY & RENEWABLE ENERGY
BIOENERGY TECHNOLOGIES OFFICE

Introduction

- Promising bioenergy technologies often *fail at scale-up*

- Modeling can guide engineers moving from bench to pilot
  - Simultaneous transport phenomena at multiple scales

- Multiscale frameworks enable the use of DOE's high-performance computing (HPC) capacity

- In this work, we apply multi-scale modeling to catalytic fast pyrolysis vapor phase upgrading over platinum on titania

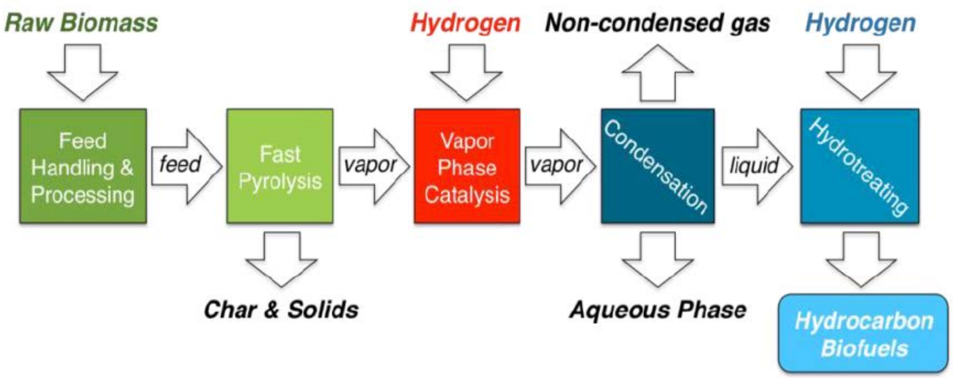

Multiscale phenomena in catalysis

molecular structure of catalytic sites dictates reactivity, selectivity, and deactivation behavior

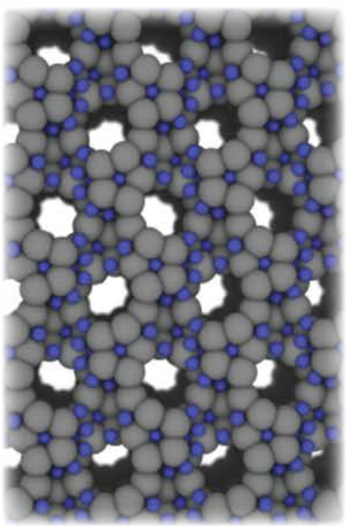

atomic scale

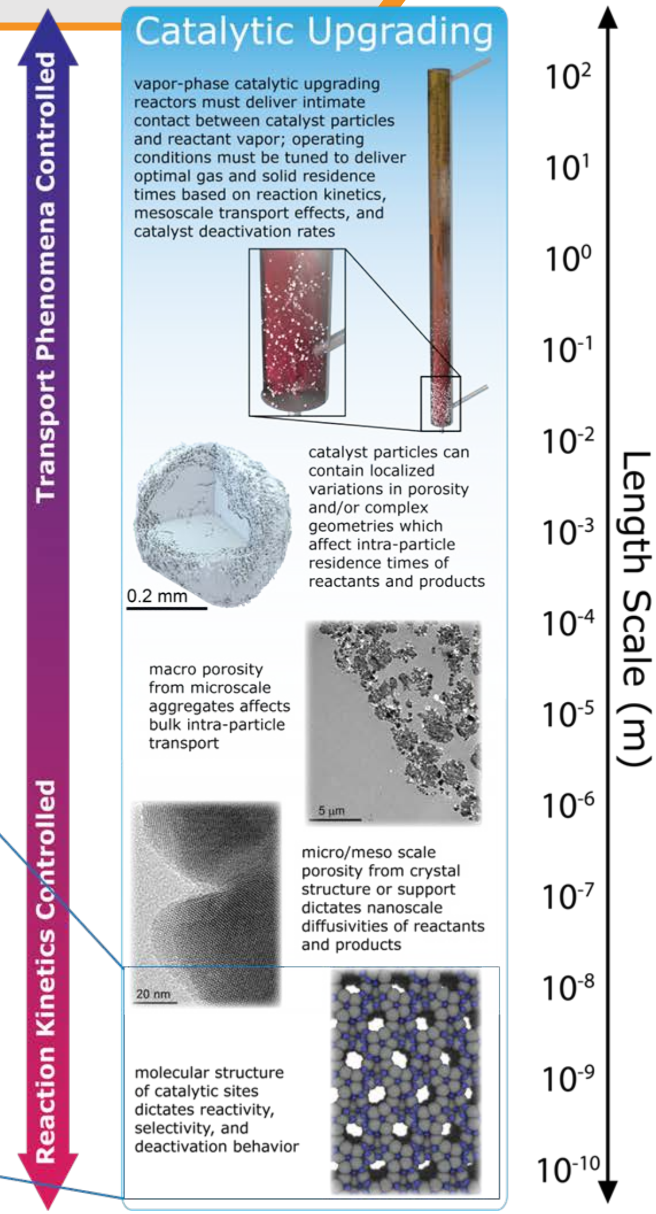

Ciesielski, Pecha, Bharadwaj, et al., Advancing catalytic fast pyrolysis through integrated multiscale modeling and experimentation: Challenges, progress, and perspectives. *Wiley Interdisciplinary Reviews: Energy and Environment* **2018,** *7,* 297.

Multiscale phenomena in catalysis

micro/meso scale porosity from crystal structure or support dictates nanoscale diffusivities of reactants and products

micro/mesopore scale

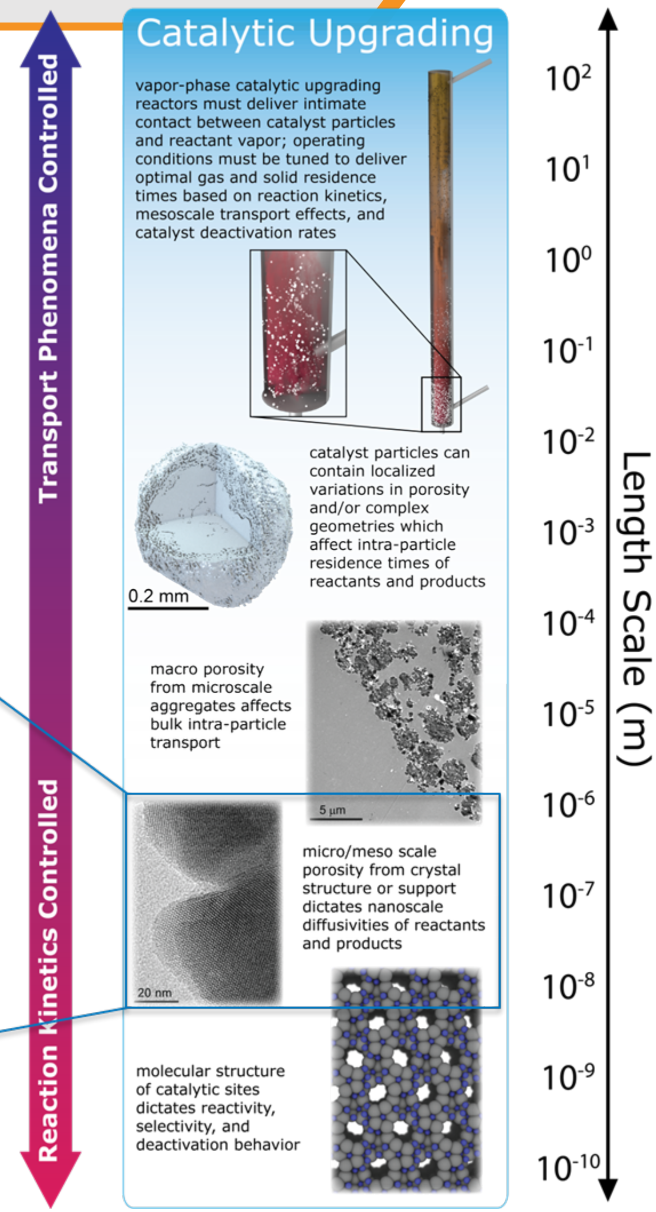

Ciesielski, Pecha, Bharadwaj, et al., Advancing catalytic fast pyrolysis through integrated multiscale modeling and experimentation: Challenges, progress, and perspectives. *Wiley Interdisciplinary Reviews: Energy and Environment* **2018,** *7,* 297.

Multiscale phenomena in catalysis

macro porosity from microscale aggregates affects bulk intra-particle transport

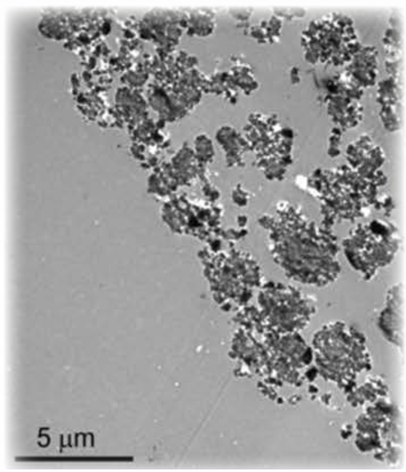

macropore scale

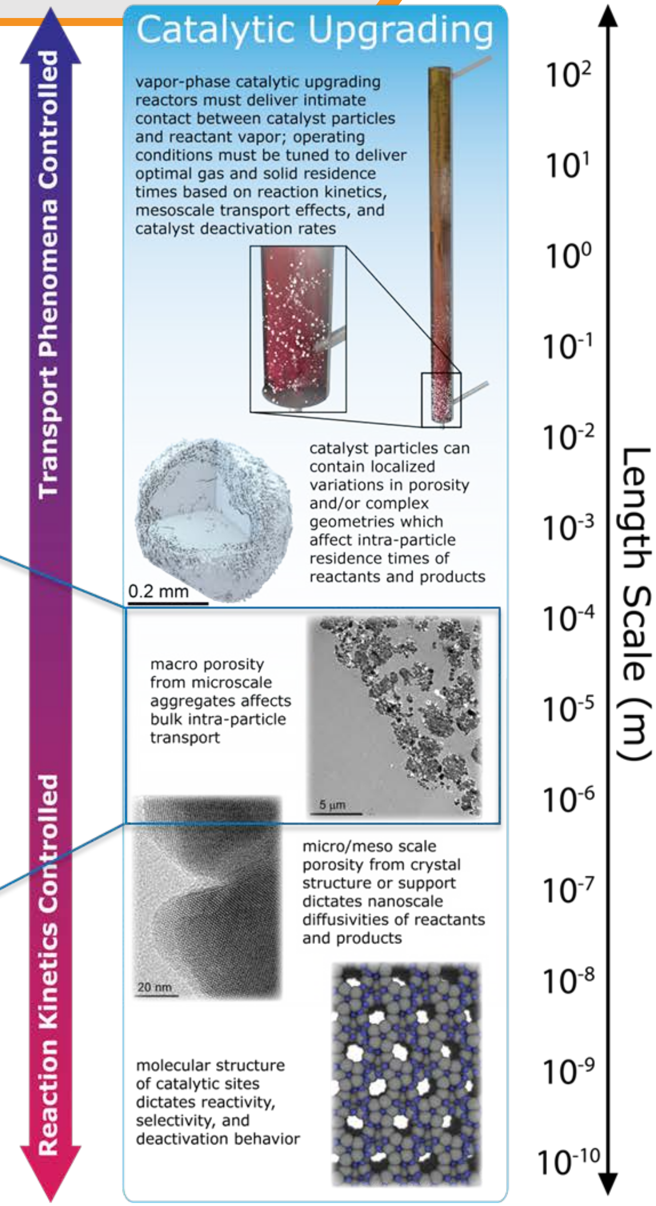

Ciesielski, Pecha, Bharadwaj, et al., Advancing catalytic fast pyrolysis through integrated multiscale modeling and experimentation: Challenges, progress, and perspectives. *Wiley Interdisciplinary Reviews: Energy and Environment* **2018,** *7,* 297.

Multiscale phenomena in catalysis

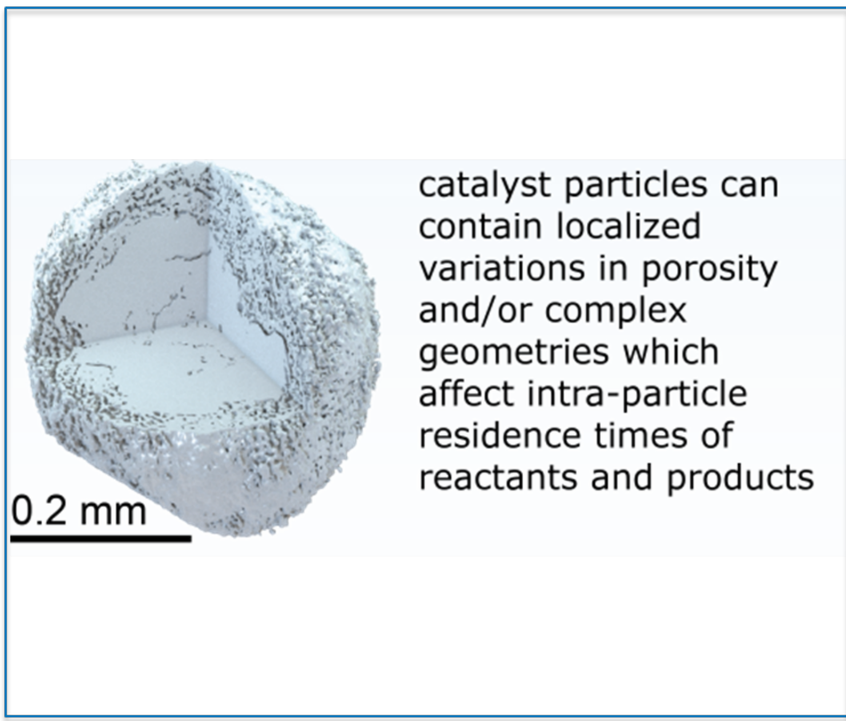

particle scale

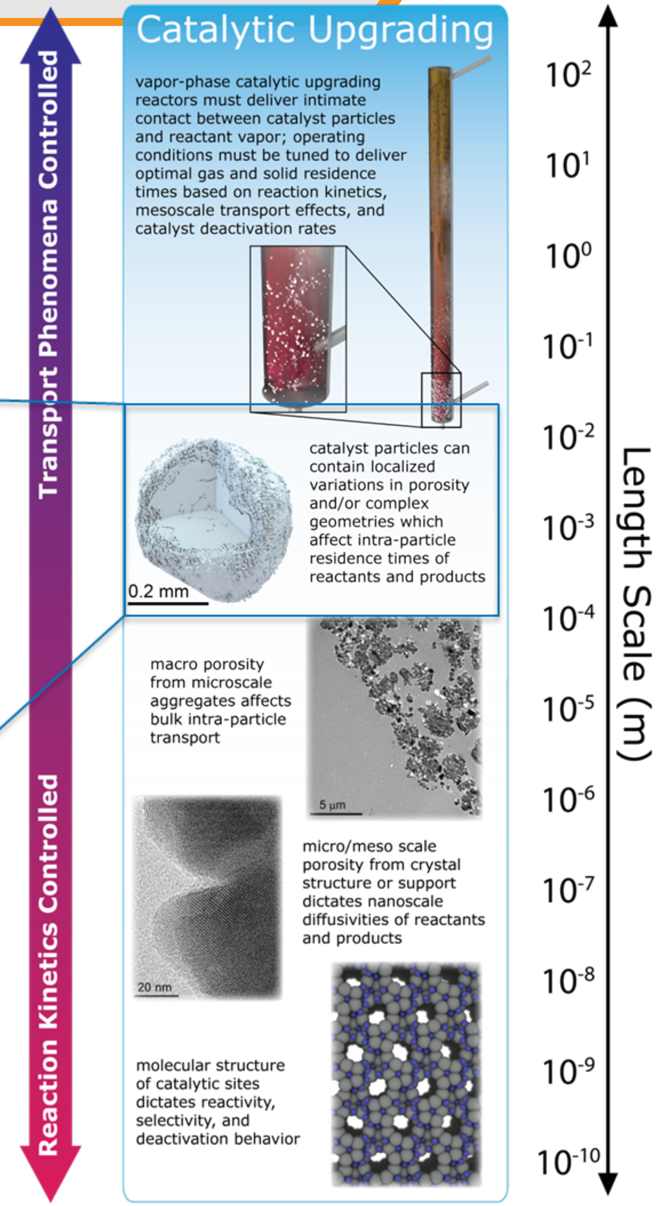

Ciesielski, Pecha, Bharadwaj, et al., Advancing catalytic fast pyrolysis through integrated multiscale modeling and experimentation: Challenges, progress, and perspectives. *Wiley Interdisciplinary Reviews: Energy and Environment* **2018,** *7,* 297.

Multiscale phenomena in catalysis

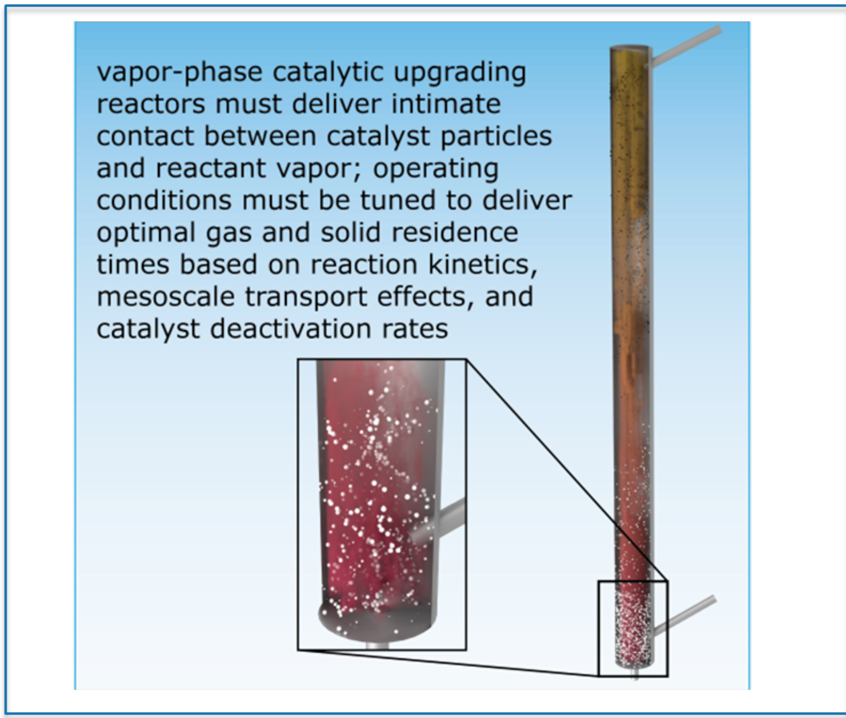

reactor scale

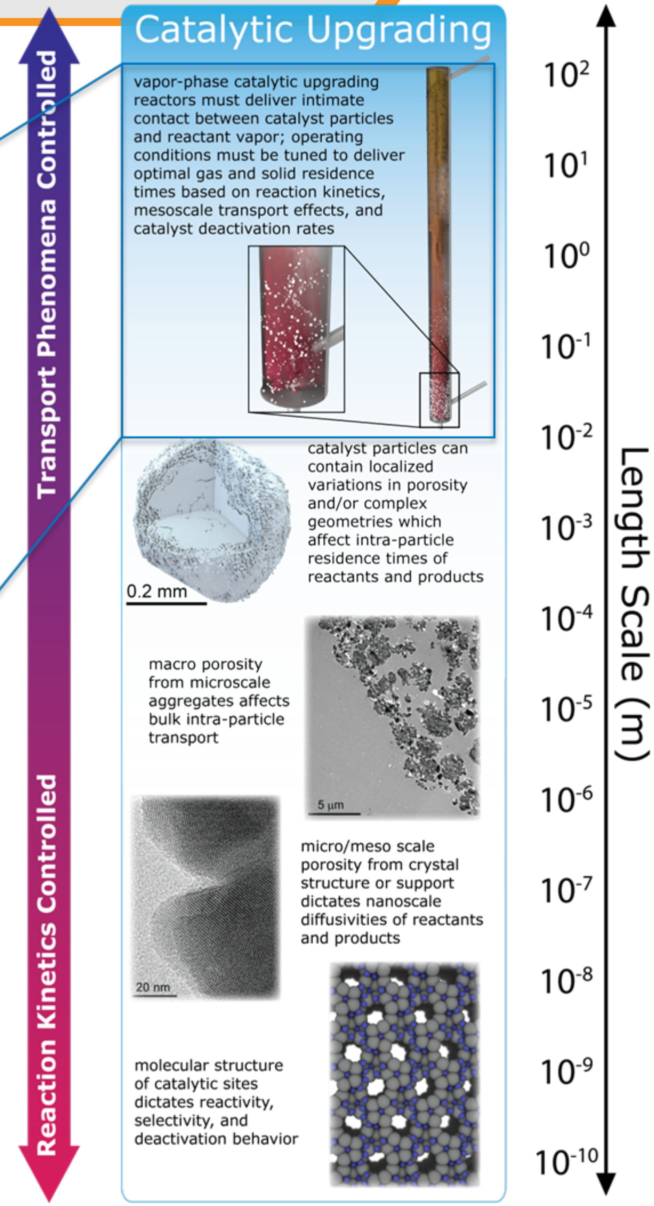

Ciesielski, Pecha, Bharadwaj, et al., Advancing catalytic fast pyrolysis through integrated multiscale modeling and experimentation: Challenges, progress, and perspectives. *Wiley Interdisciplinary Reviews: Energy and Environment* **2018,** *7,* 297.

Observed reaction rate: Physics at all scales

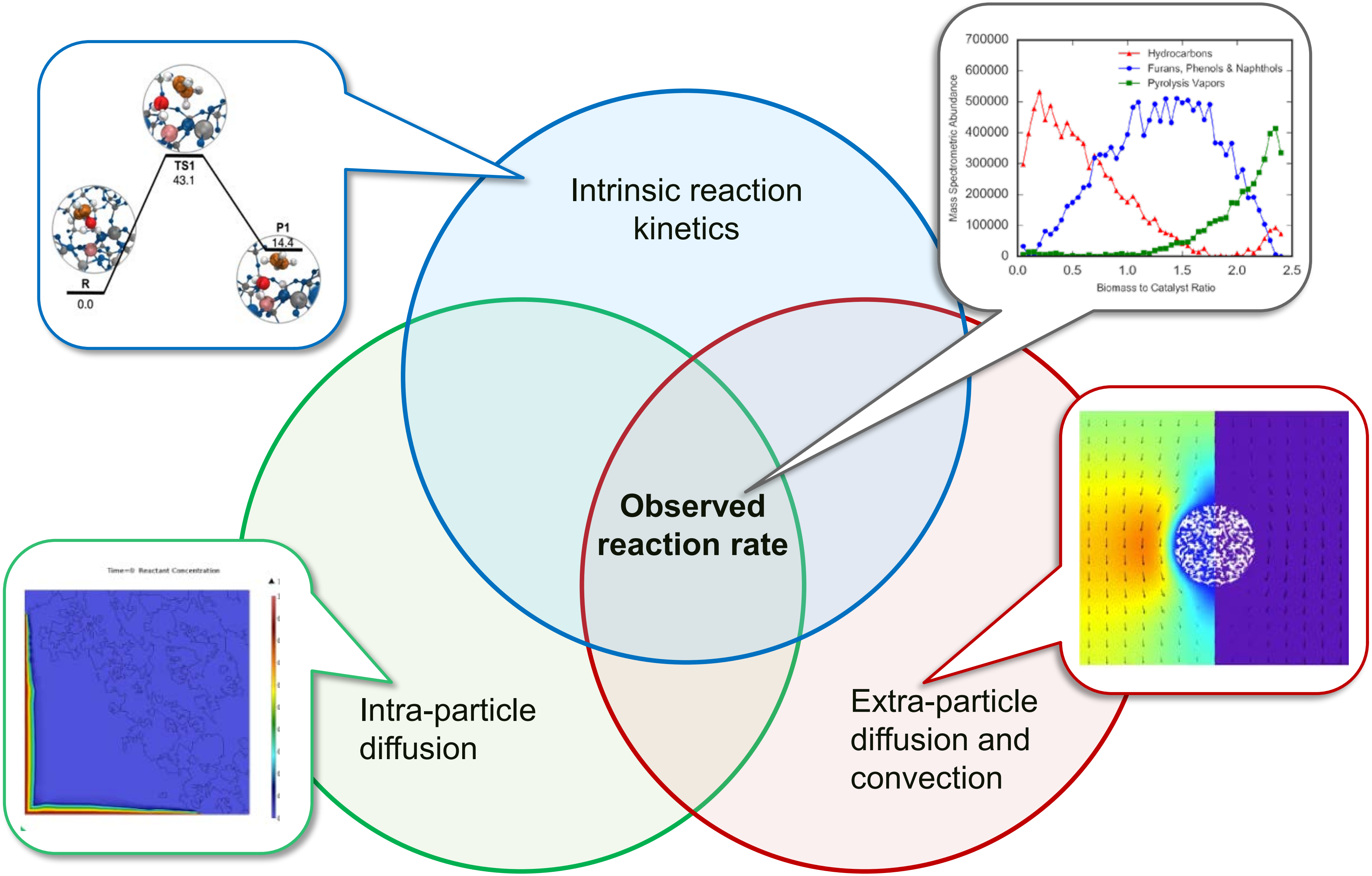

Experimental setup for CFP

Bench scale *ex-situ* catalytic fast pyrolysis system utilized in this work with a packed bed (fixed bed) of catalyst

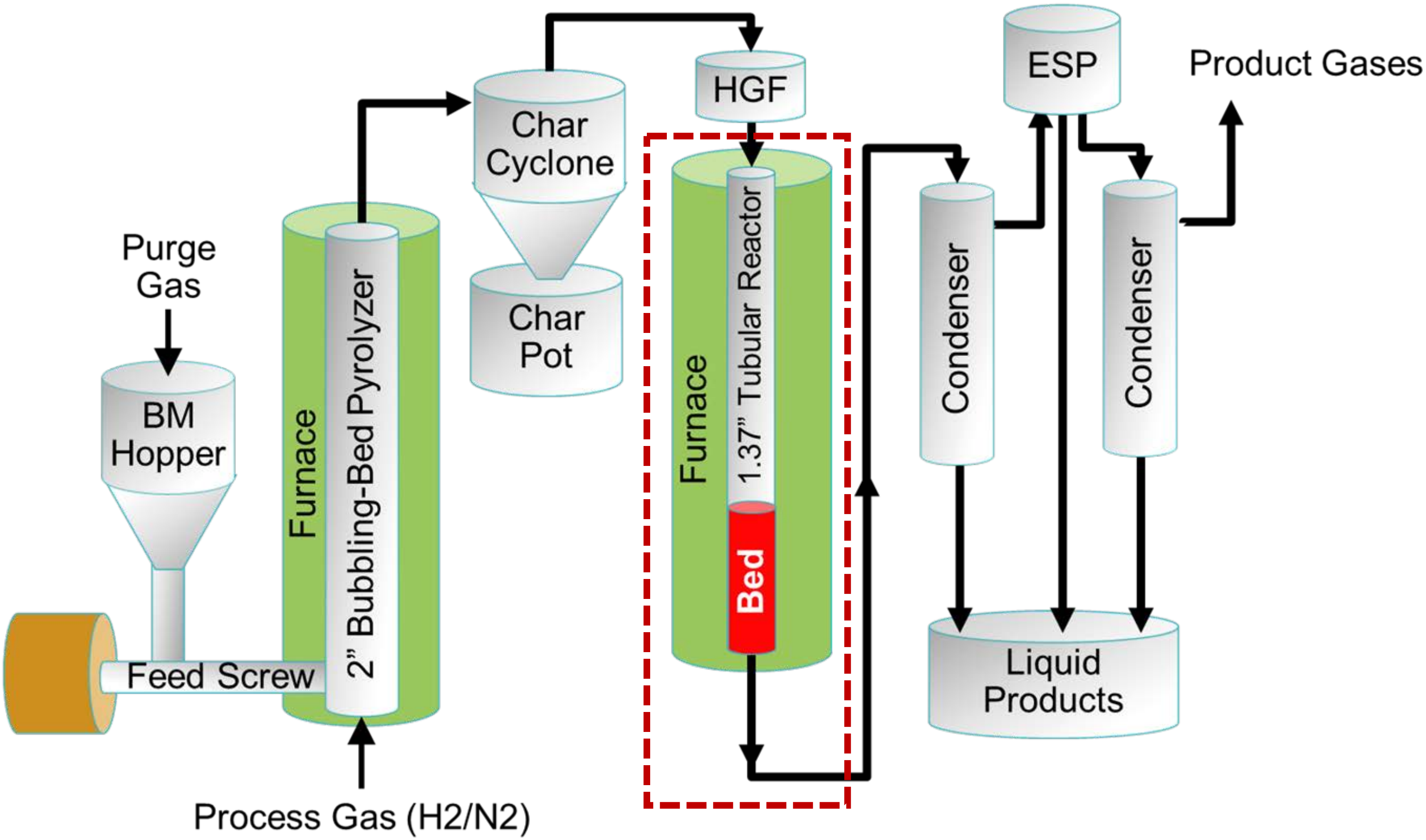

Problem description

Packed bed vapor phase upgrading reactor

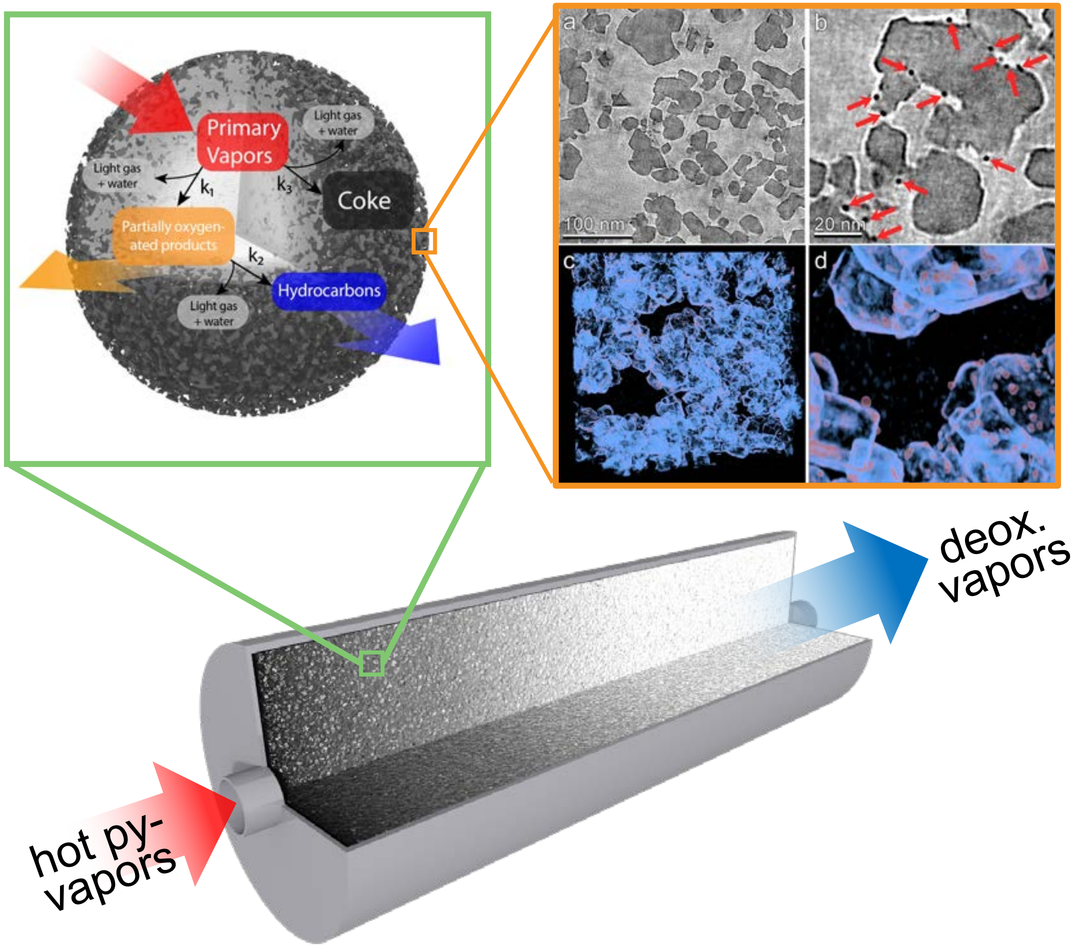

Pecha, Iisa, Griffin, Mukarakate, French, Adkins, Bharadwaj, Crowley, Foust, Schaidle, and Ciesielski. "Ex situ upgrading of pyrolysis vapors over PtTiO 2: extraction of apparent kinetics via hierarchical transport modeling." *Reaction Chemistry and Engineering*, **2020**

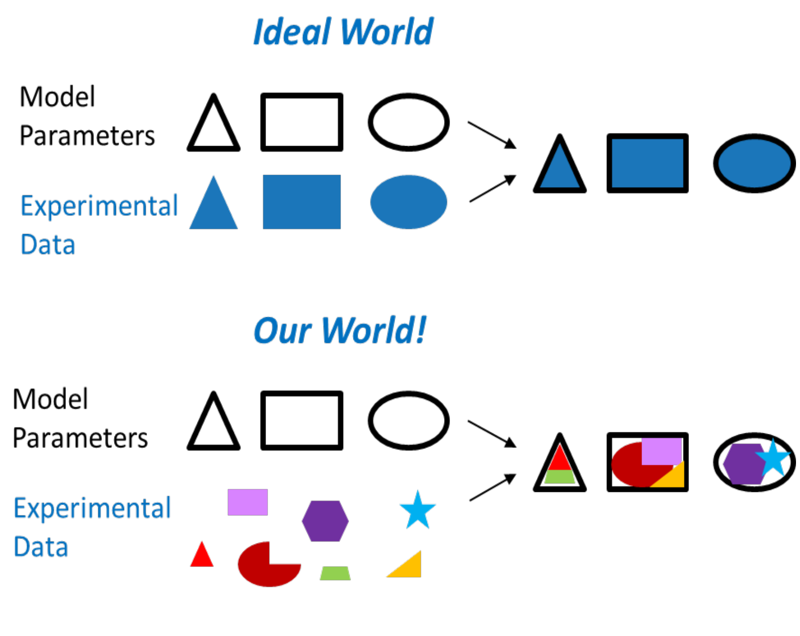

Schematic credit: Jim Parks

Relevance:

- **Coke profiles predicted by the simulation enable detailed simulation of regeneration cycles.**
- **Transport-independent kinetic parameters enable computational scaling studies and in-silico reactor optimization.**

Yields can be broken down into lumps

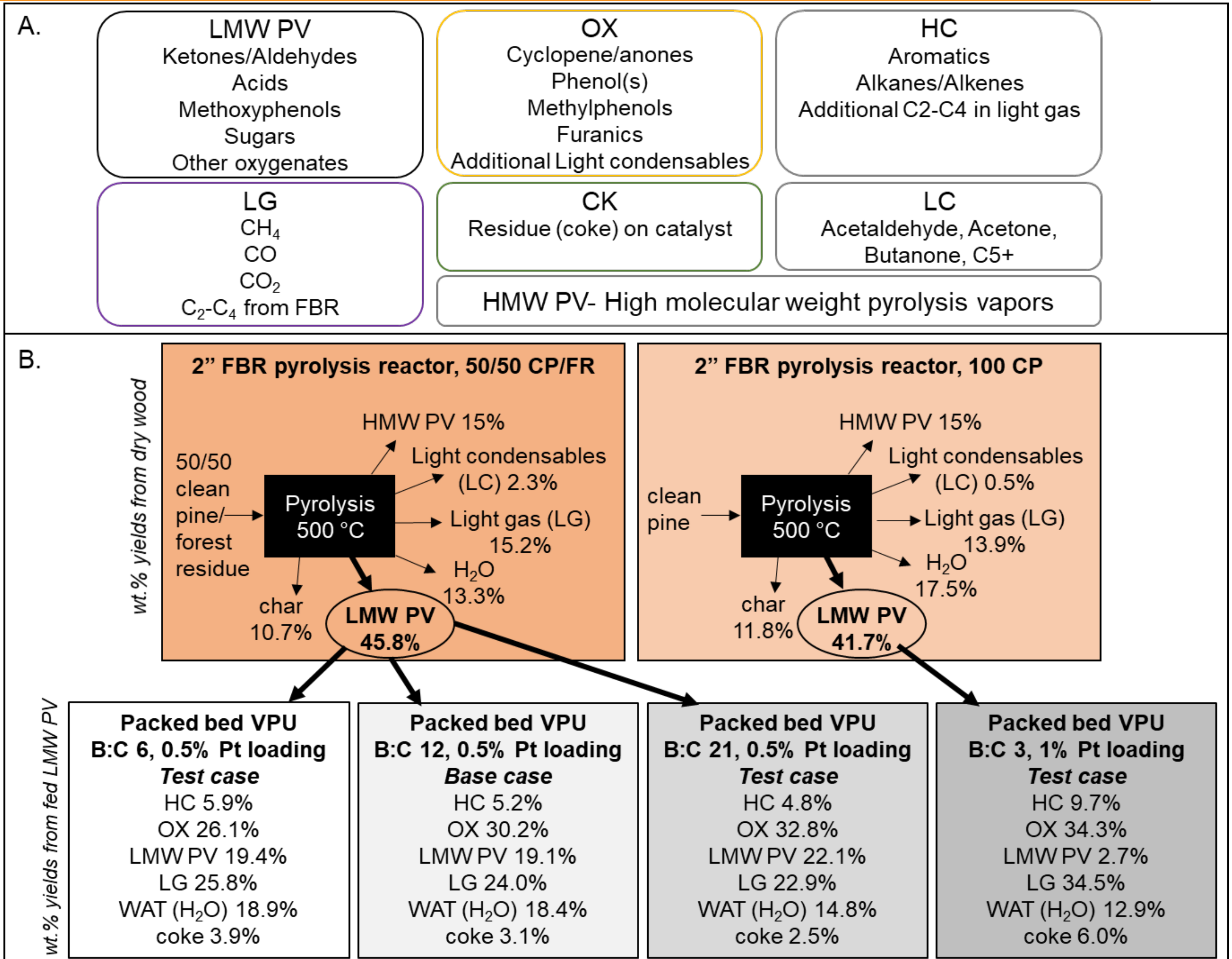

Deactivation and multiple active sites

On-stream MS shows rapid deactivation

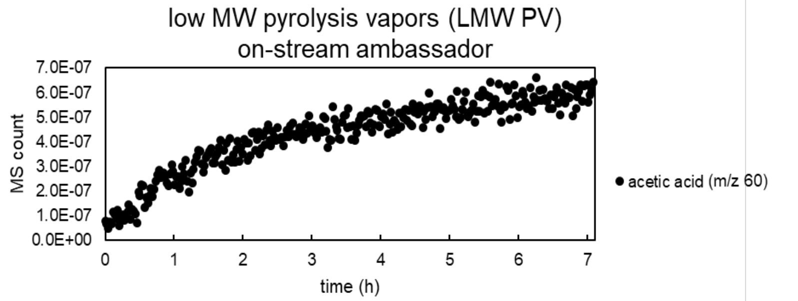

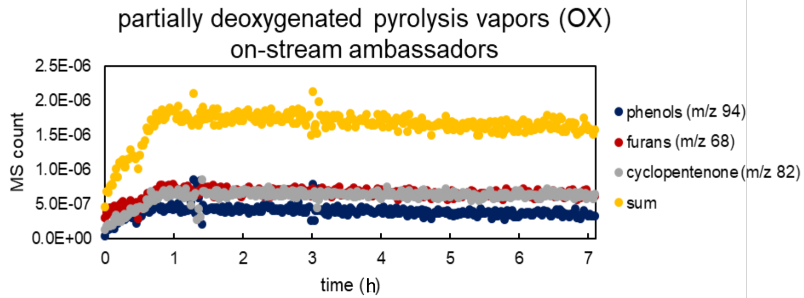

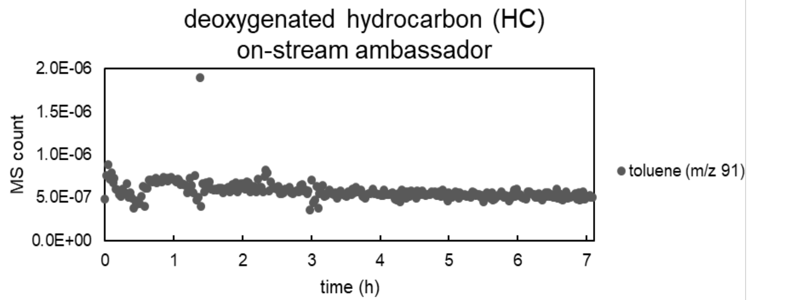

Lumped reaction scheme describes organic fraction of pyrolysis vapors over PtTiO2

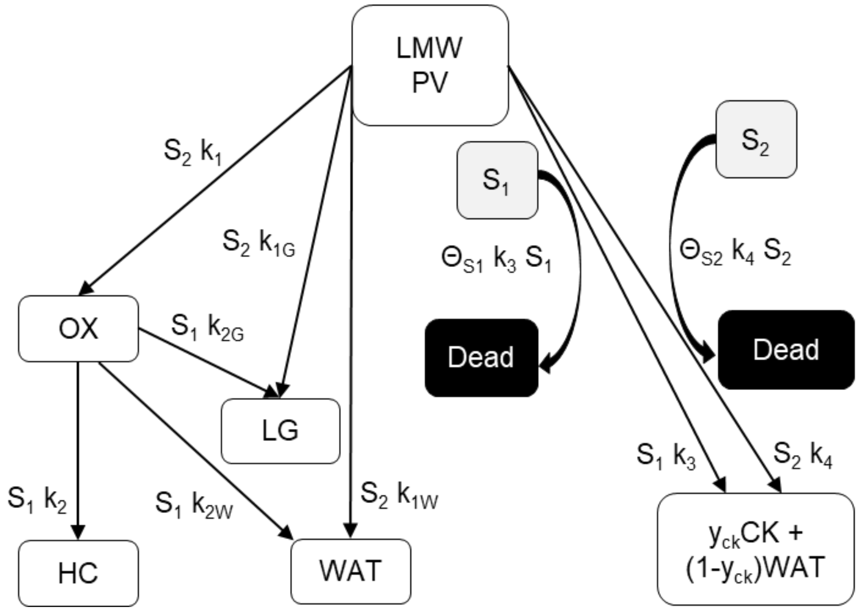

How do changes to catalyst properties and operating conditions impact process performance metrics (yield, composition, catalyst lifetime)?

Modeling approach: Extending the Thiele effectiveness factor

Problem: Accurately model multi-step reactions requires heavy computational resources, not suitable for iterative parameter extraction

Hypothesis: An analytical solution to diffusion-reaction-deactivation is mathematically feasible and will accurately represent multi-step reactions

Solution: Extend the effectiveness factor

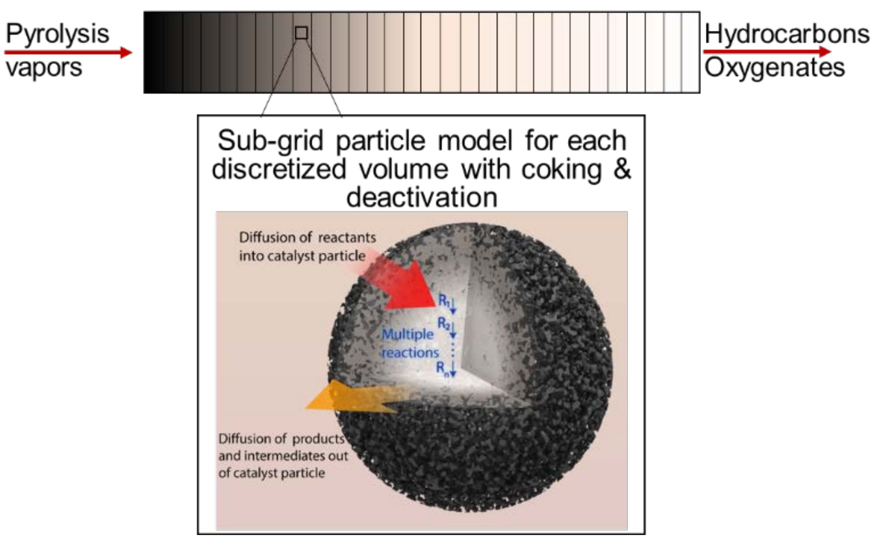

State of the art for accounting for diffusion limitations in porous catalysts: Thiele (1930s) + Aris (1970s)

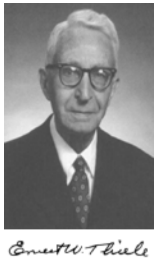

$$\phi = \sqrt{\frac{ka^2}{D_{\mathrm{eff}}}}$$

$$\eta = \frac{3C_{Bi}}{\phi^2}\left(\phi\coth(\phi) - 1\right)$$

$$C_{Bi} = \frac{Bi}{\left(\phi\coth(\phi) - 1 + Bi\right)}$$

***No** coupling of intraparticle sequential reactions*

Extending the Thiele effectiveness factor: A bridge between scales

1) Unsteady advection-diffusion-reaction

$$\frac{\partial C_i}{\partial t} + \mathbf{u} \cdot \Delta(C_i) = \Delta \cdot \mathbf{J}_i - \sum_{j=1}^{N} \dot{r}_{ij} + \sum_{m=1}^{N} \dot{r}_{im}$$

2) Assume no advection, sphere

$$\frac{\partial C_i}{\partial t} = \frac{1}{r^2}\frac{\partial}{\partial r}\left(r^2 D_{i,\text{eff}} \frac{\partial C_i}{\partial r}\right) - \sum_{j=1}^{N} \dot{r}_{ij} + \sum_{m=1}^{N} \dot{r}_{im}$$

3) Nondimensionalize, cons. & prod. TM

$$\hat{C}_i = \frac{C_i}{C_{1,\infty}} \qquad \hat{r} = \frac{r}{R_p} \qquad \hat{t}_i = t\frac{D_{i,\text{eff}}}{R_p^2}$$

$$\phi_i = \sqrt{\frac{R_p^2 \psi^t \sum_{j=1}^{N} k_{ij}}{D_{i,\text{eff}}}} \qquad \phi_{im} = \sqrt{\frac{R_p^2 \psi^t k_{im}}{D_{i,\text{eff}}}}$$

4) Quasi-steady state + BCs in sphere (Ω)

$$\frac{d^2\hat{C}_i}{d\hat{r}^2} + \frac{2}{\hat{r}}\frac{d\hat{C}_i}{d\hat{r}} - \phi_i^2 \hat{C}_i = -\sum_{m}^{N} \phi_{im}^2 \hat{C}_m \qquad \text{in } \Omega$$

$$\frac{d\hat{C}_i}{d\hat{r}} = 0 \qquad \text{on } \partial\Omega_1$$

$$\frac{d\hat{C}_i}{d\hat{r}} = Bi\left(1 - \hat{C}_i\right) \qquad \text{on } \partial\Omega_2$$

5) Use matrix-vector form (matrix of Thiele moduli for consumption-production)

$$\frac{d^2\hat{\mathbf{C}}}{d\hat{r}^2} + \frac{2}{\hat{r}}\frac{d\hat{\mathbf{C}}}{d\hat{r}} - \bar{\phi}^2\hat{\mathbf{C}} = 0$$

Lattanzi A, Pecha MB, Bharadwaj VS, Ciesielski PN, "Beyond the effectiveness factor: multi-step reactions with intraparticle diffusion limitations," *Chemical Engineering Journal* (2020) 380, 15, 122507.

Extending the Thiele effectiveness factor: A bridge between scales

6) When eigenvalues (λ) are real, solution is hyperbolic function

$$\hat{U}_i = A_1 \sinh(\sqrt{\lambda_i}\hat{r}) + A_2 \cosh(\sqrt{\lambda_i}\hat{r}) \qquad \lambda_i > 0$$

7) Converting back to concentration & BCs (P is eigenvector matrix)

$$\hat{\mathbf{C}} = \bar{\mathbf{P}}\bar{\mathbf{D}} \left(\frac{C_{Bi} \sinh\left(\sqrt{\lambda}\hat{r}\right)}{\sinh\left(\sqrt{\lambda}\right)\hat{r}} \right) \bar{\mathbf{P}}^{-1} \hat{\mathbf{C}}_{\mathrm{Rat},\infty}$$

8) Volume-averaging the rates

$$< \dot{r}_{ij} >\equiv \frac{4\pi R_p^3 \psi k_{ij} C_{1,\infty}}{4/3\pi R_p^3} \int_0^1 \hat{C}_i \hat{r}^2 \, d\hat{r} = \psi k_{ij} C_{1,\infty} \eta_i,$$

9) Multi-step effectiveness vector! (MEV)

$$\boldsymbol{\eta} = \bar{\mathbf{P}}\bar{\mathbf{D}} \left(\frac{3C_{Bi}}{\lambda} \left(\sqrt{\lambda} \coth(\sqrt{\lambda}) - 1 \right) \right) \bar{\mathbf{P}}^{-1} \hat{\mathbf{C}}_{\mathrm{Rat},\infty}$$

10) Individual rates with MEV!

$$< \dot{r}_i >\equiv \sum_m < \dot{r}_{im} > - \sum_j < \dot{r}_{ij} >= \psi C_{1,\infty} \left(\sum_m k_{im} \eta_m - \sum_j k_{ij} \eta_i \right)$$

Lattanzi A, Pecha MB, Bharadwaj VS, Ciesielski PN, "Beyond the effectiveness factor: multi-step reactions with intraparticle diffusion limitations," *Chemical Engineering Journal* (2020) 380, 15, 122507.

Apply multistep effectiveness vector to PBR

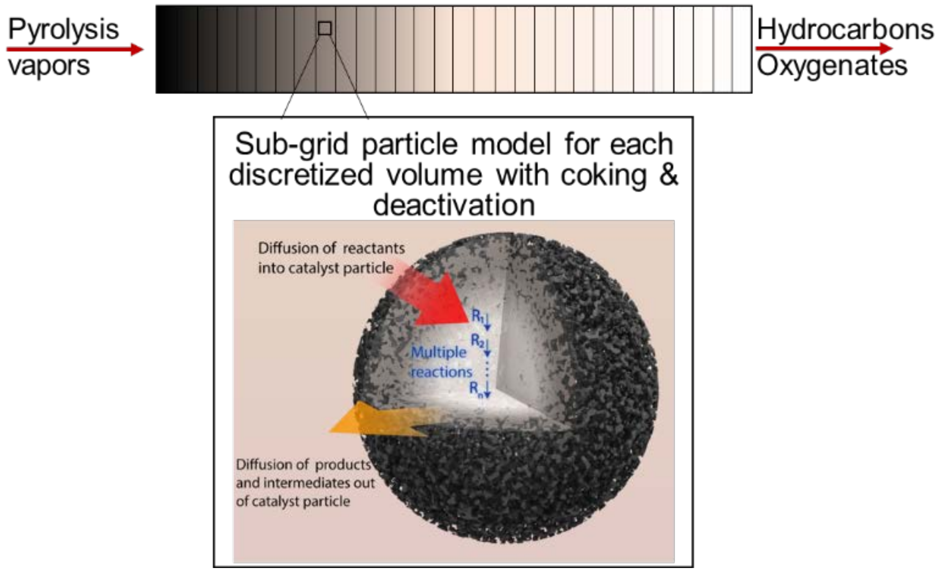

Apparent rate equations inside MEV formulation

$$R_1 = PV_{LMW} k_1 S_2$$
$$R_{1G} = PV_{LMW} k_{1G} S_2$$
$$R_{1W} = PV_{LMW} k_{1W} S_2$$
$$R_2 = OX\ k_2 S_1$$
$$R_{2G} = OX\ k_{2G} S_1$$
$$R_{2W} = OX\ k_{2W} S_1$$
$$R_3 = PV_{LMW} k_3 S_1$$
$$R_4 = PV_{LMW} k_4 S_2$$

Packed bed transport equations

$$\frac{\partial PV_{LMW}}{\partial t} = -u\frac{\partial PV_{LMW}}{\partial x} + D_{PV}\frac{\partial^2 PV_{LMW}}{\partial x^2} - R_{PV_{LMW},eff}\left(1-\varepsilon_p\right)$$
$$\frac{\partial OX}{\partial t} = -u\frac{\partial OX}{\partial x} + D_{OX}\frac{\partial^2 OX}{\partial x^2} - R_{OX,eff}\left(1-\varepsilon_p\right)$$
$$\frac{\partial HC}{\partial t} = -u\frac{\partial HC}{\partial x} + D_{HC}\frac{\partial^2 HC}{\partial x^2} - R_{HC,eff}\left(1-\varepsilon_p\right)$$
$$\frac{\partial LG}{\partial t} = -u\frac{\partial LG}{\partial x} + D_{LG}\frac{\partial^2 LG}{\partial x^2} - R_{LG,eff}\left(1-\varepsilon_p\right)$$
$$\frac{\partial WAT}{\partial t} = -u\frac{\partial WAT}{\partial x} + D_{WAT}\frac{\partial^2 WAT}{\partial x^2} - R_{WAT,eff}\left(1-\varepsilon_p\right)$$
$$\frac{\partial S1}{\partial t} = R_{S1,eff}\left(1-\varepsilon_p\right)$$
$$\frac{\partial S2}{\partial t} = R_{S2,eff}\left(1-\varepsilon_p\right)$$
$$\frac{\partial CK}{\partial t} = R_{CK,eff}\left(1-\varepsilon_p\right)$$
$$PV_{LMW} = PV_{LMW,0},\ x = 0$$
$$HC = OX = LG = WAT = 0,\ x = 0$$
$$\frac{dPV}{dt} = \frac{dOX}{dt} = \frac{dHC}{dt} = \frac{dLG}{dt} = \frac{dWAT}{dt} = 0,\ x/L = 1$$

Catalyst characterization

Multiscale imaging of the Pt/TiO2 catalyst particles

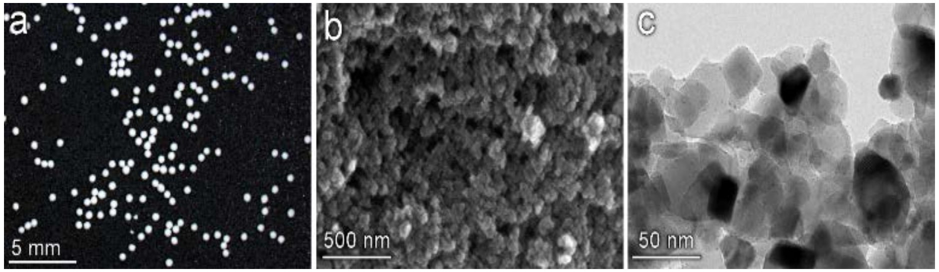

(a) Light microscopy of catalyst particles showing the spherical bulk geometry with narrow size distribution. (b) Scanning electron microscopy (SEM) of the particle surface reveals a porous support structure formed by the agglomeration of TiO2 nanoparticles. (c) Transmission electron microscopy shows the presence of ~5 nm Pt particles visualized as dark spots on the surface of the larger TiO_2 support structure.

TEM Tomography of the TiO_2 catalyst particle mesostructure

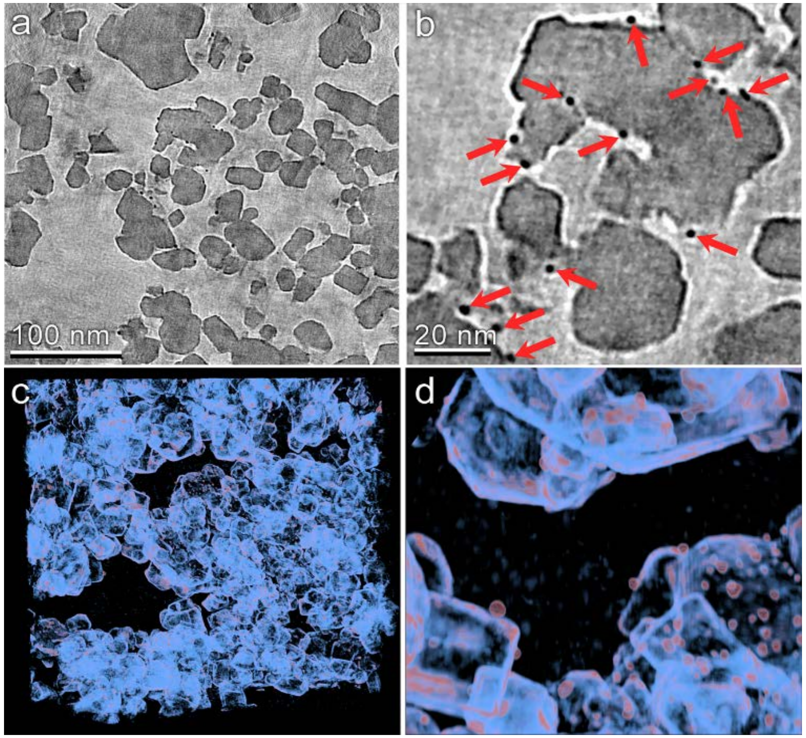

(**a, b**) Slices through the tomographic volume are shown at two different magnifications. Pt particles are clearly identified by their higher electron density (indicated by red arrows in panel b). (**c, d**) 3D visualizations of the reconstructed volume are shown at two different magnifications.

Apparent rate constants fit to real data

Initial guess for 10 apparent rate parameters + experimental data

Simplex parameter optimizer + PBR model

New parameters from optimizer

Multiscale packed bed model

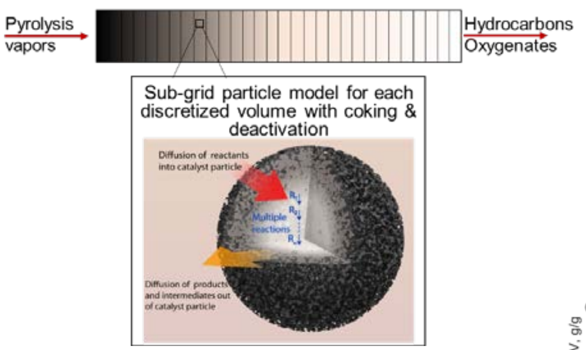

Objective function (yield vs time)

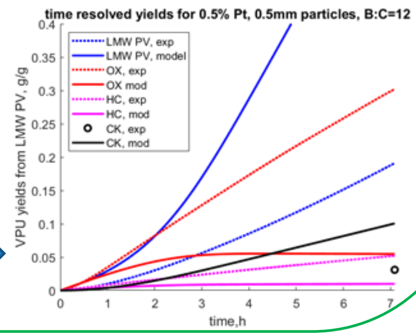

Best-fit lumped rate constants fit for base case

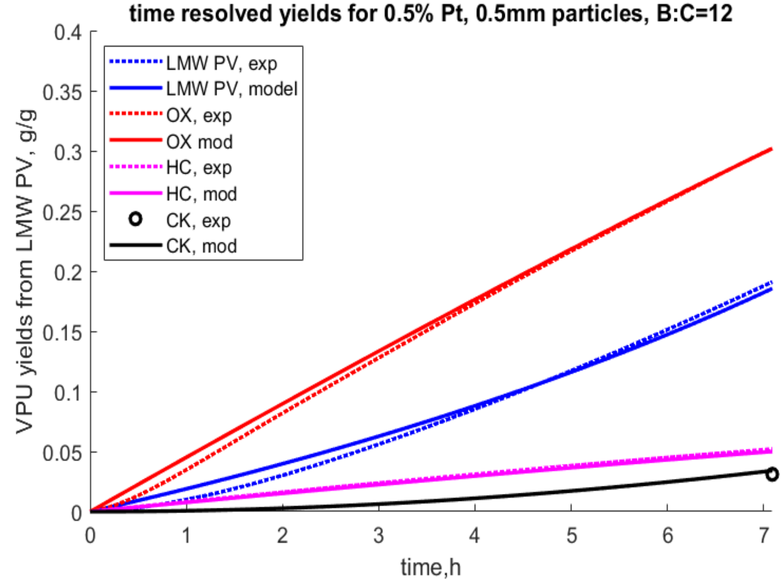

RATE CONSTANT	FITTED VALUE
k1 [s^{-1}]	76
k1g [s^{-1}]	50.5
k1w [s^{-1}]	39
k2 [s^{-1}]	5.4
k2g [s^{-1}]	0.7
k2w [s^{-1}]	7.9E-10
k3 [s^{-1}]	7E-14
k4 [s^{-1}]	3.7E-4
Θ_{S1}	1.2E-3
Θ_{S2}	15.2

Results: Model validation

Yields from low MW pyrolysis vapors, VPU only

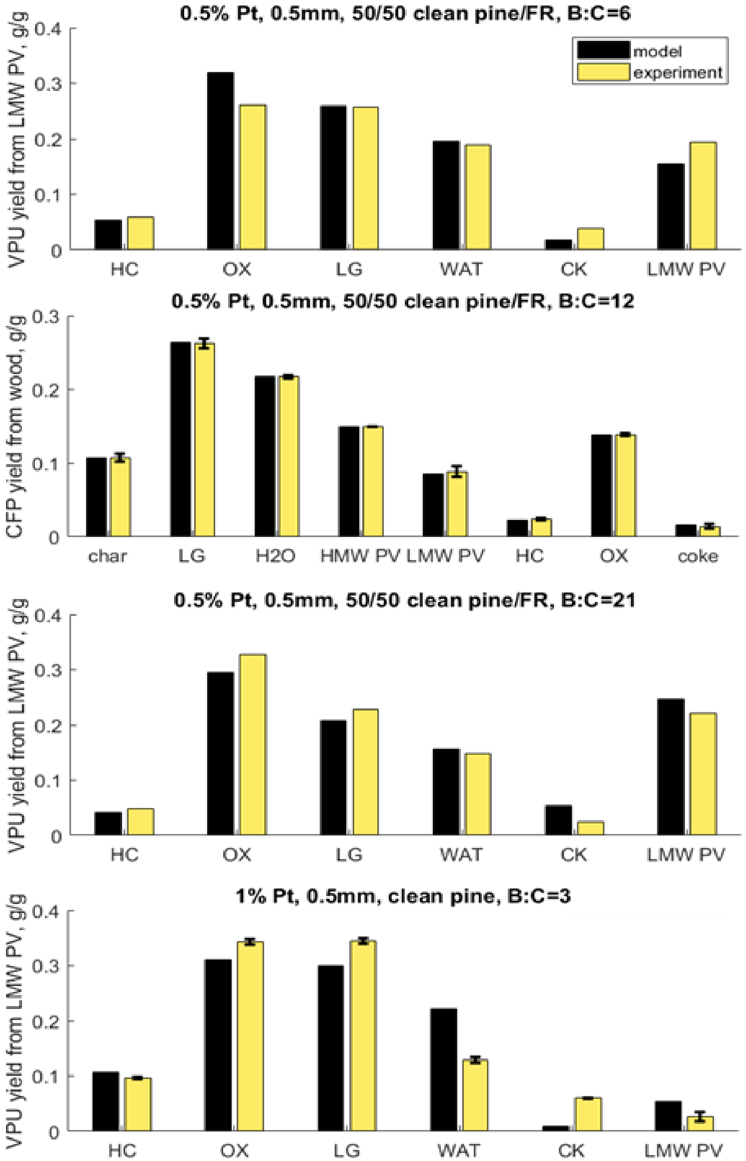

Yields from dry wood for pyrolysis + VPU

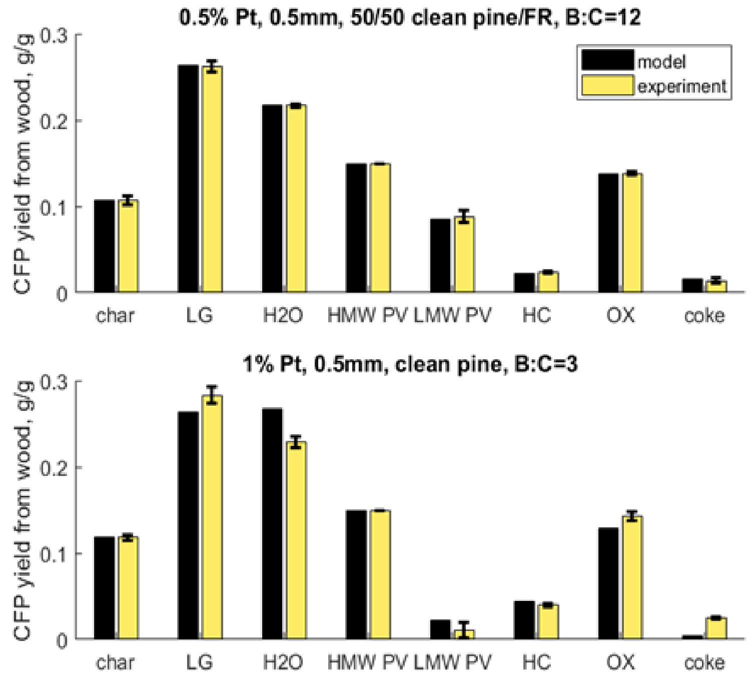

Results: Predictions and extrapolations

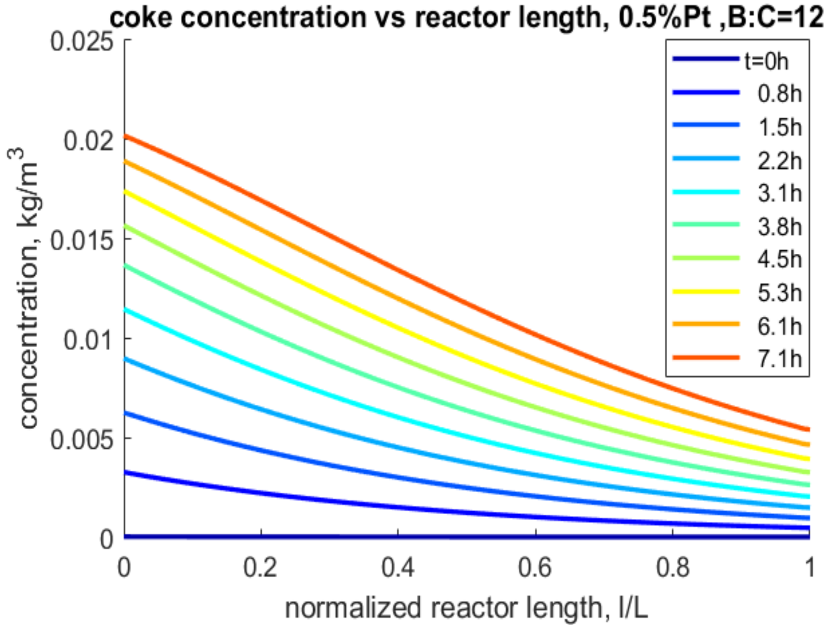

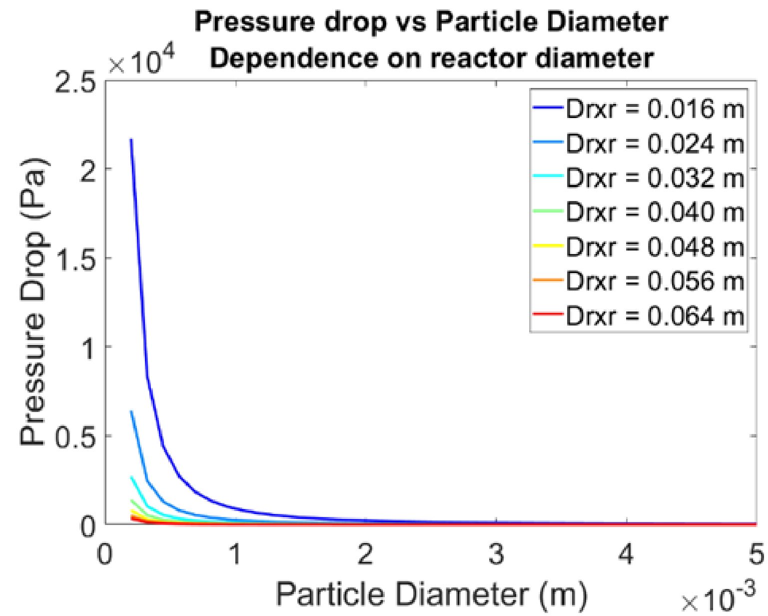

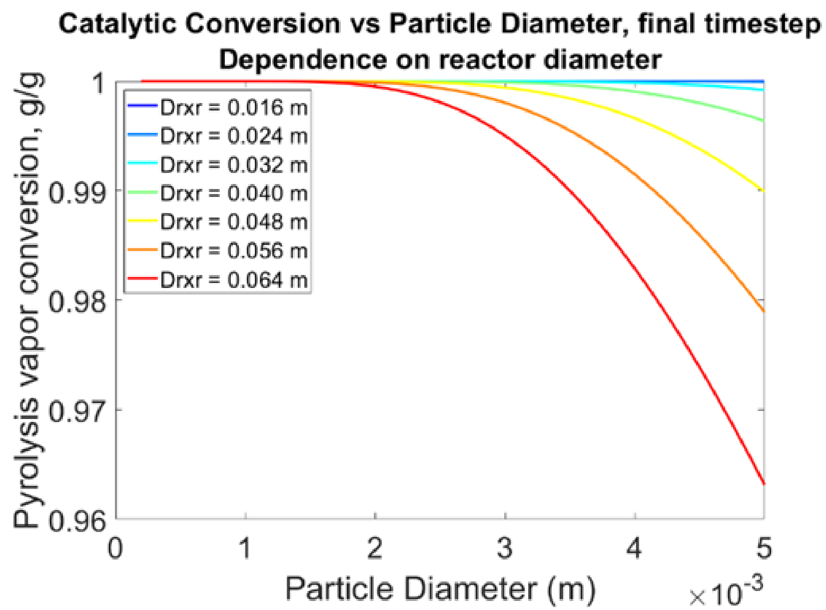

Conclusions

- New multiscale simulation framework was capable of capturing
  - multiple cascading reactions
  - multiple operating conditions
  - catalyst loadings
  - active site deactivation
- Fast, accurate, can be used to mine old *good* data
- Future work will extend the model to other catalyst shapes, other technologies
- In the next slides, you will see how results from this work were used to design a catalytic regeneration system at a much larger scale with a different set of modeling tools.

ChemCatBio
Chemical Catalysis for Bioenergy

Packed Bed Reactor Scale-up Using High Fidelity Reactor Models

U.S. DEPARTMENT OF ENERGY | Office of ENERGY EFFICIENCY & RENEWABLE ENERGY
BIOENERGY TECHNOLOGIES OFFICE

Lab Scale Packed Bed Reactor (PBR) and Catalyst

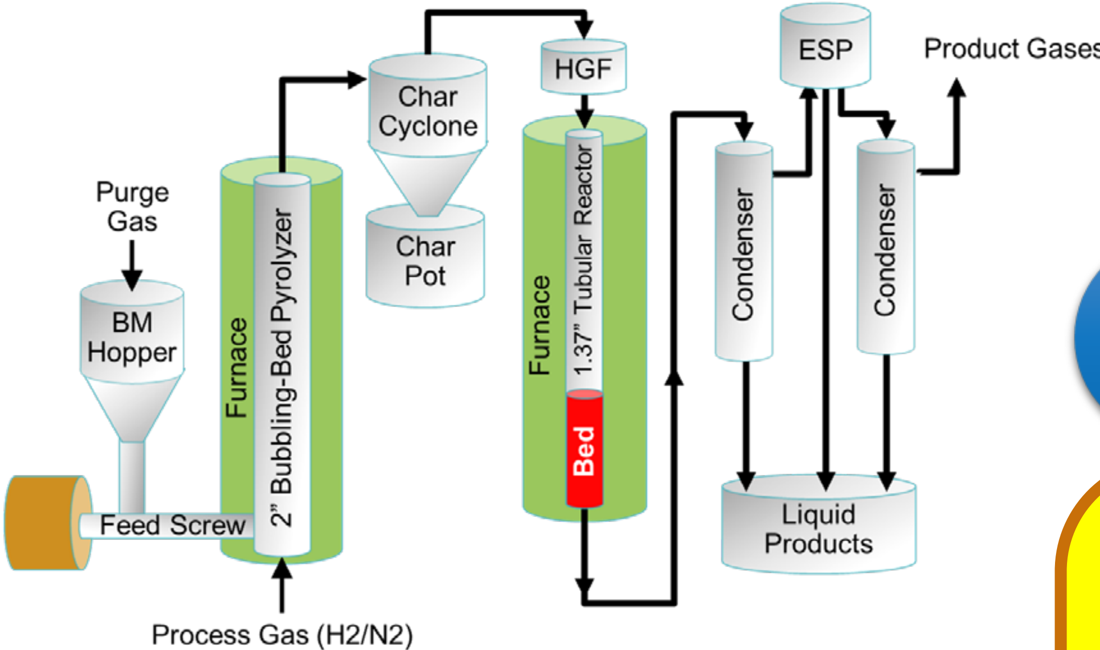

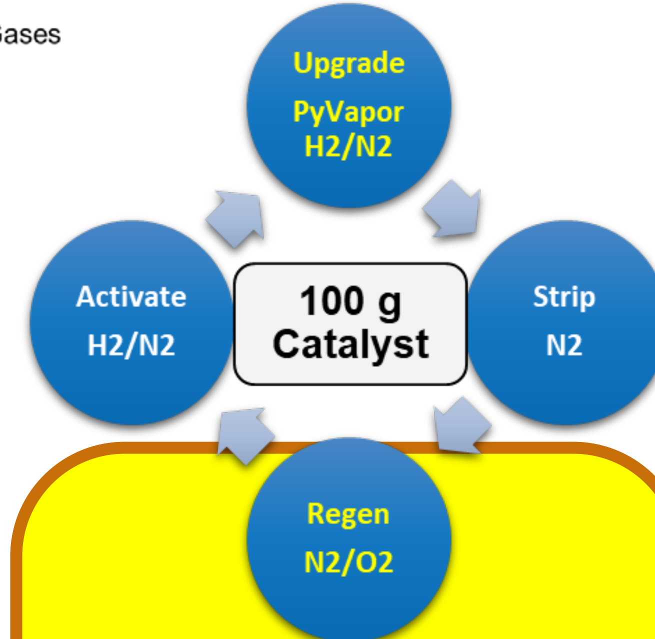

0.5 mm Pt/TiO_2 Spheres

Upgrading	
Biomass Feed, g/hr	150
Inlet Pressure, kPa	110
Inlet Temperature, °C	410
H2 Flowrate, SLPM	13.5
N2 Flowrate, SLPM	2.4
WHSV, hr^{-1}	1.5
Duration, B/C (hr)	12 (8)

Oxidative Regeneration	
Inlet Temperature, °C	410
Outlet Temperature, °C	450
N2 Flowrate, SLPM	15.6
Air Flowrate, SLPM	0.42
Duration, hr	8

Scaling Up the PBR

- TCPDU-PBR
  - 6 kg cat
  - 9 kg/hr biomass
  - WHSV 1.5 hr^{-1}
- Constraints
  - PBR ΔP 20 kPa or less
  - No wall heat removal (mimic industrial scale)
  - Gas temperature ≈ 400°C to minimize cycle time and ensure quick light-off
  - B/C = 12 corresponds to 25 wt% coke (g C / g fresh)

Scaling Up the PBR (2)

- Split the 6 kg bed between 3 existing reactors, 2 kg each
- Per-bed scale-up = 20 X
- N2 flow limit = 1200 SLPM, 400 per bed
- Each reactor has 3 heating rods which can be converted to cooling tubes
- Air flow limit = 1800 SLPM, 200 per tube

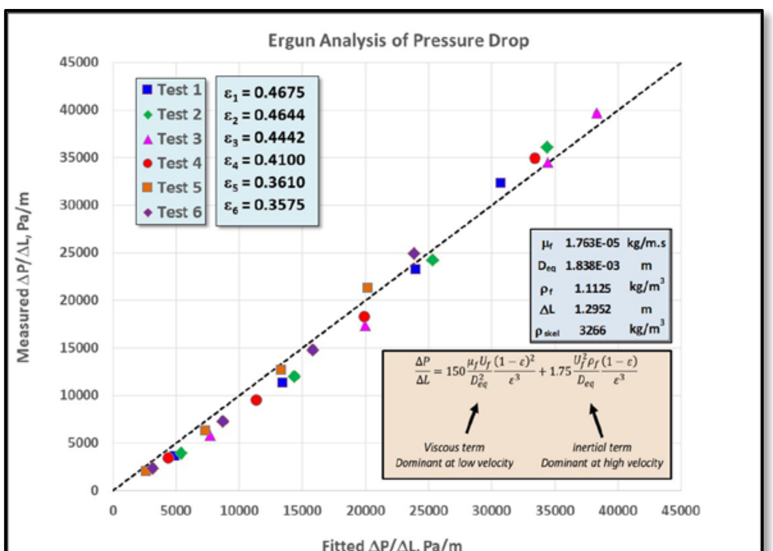

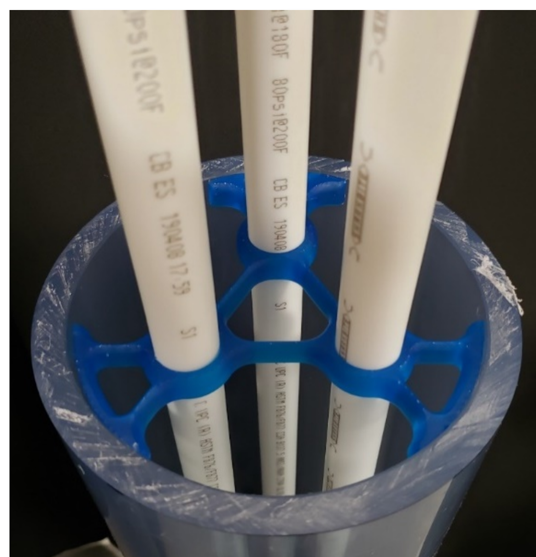

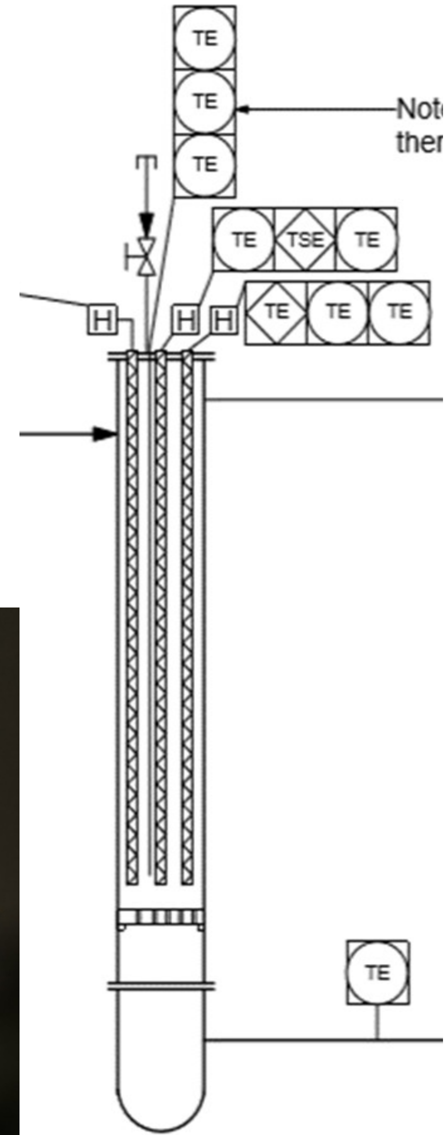

Model Details

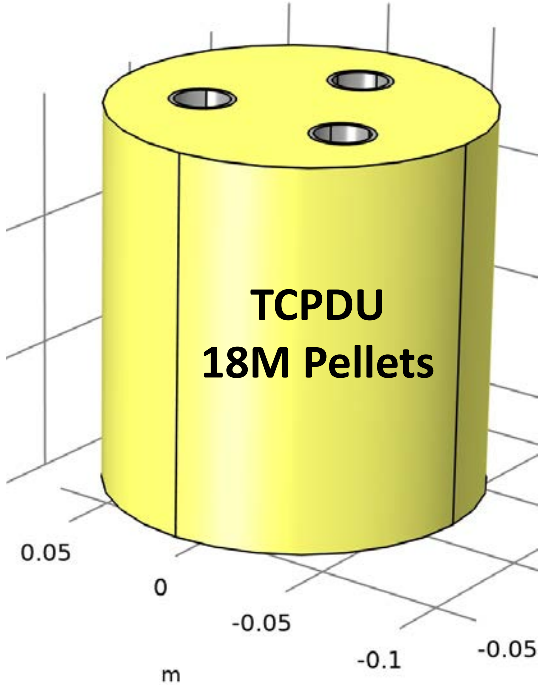

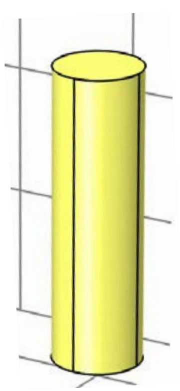

2FBR
900k Pellets

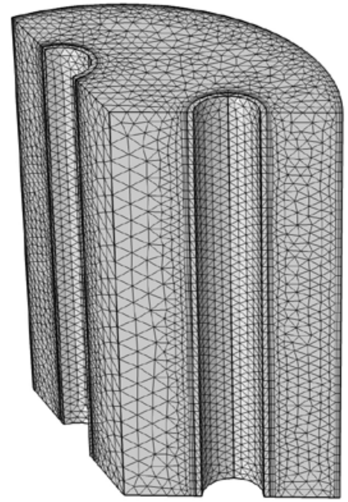

n_{cell} = 152k $n_{pellet/cell}$ = 120

n_{cell} = 434k $n_{pellet/cell}$ = 42

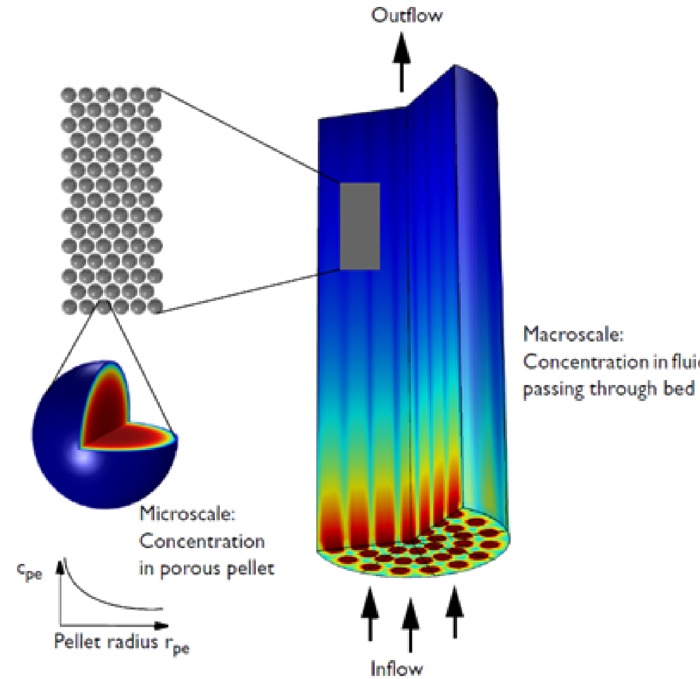

Image made using COMSOL Multiphysics® software and provided courtesy of COMSOL.[26]

N2 Flow, SLPM (410°C)	Cooling Air Flow, SLPM (30°C)		
	600	300	No Flow
400	Case 1	Case 2	Case 3
300	Case 4	Case 5	Case 6
200	Case 7	Case 8	Case 9

2FBR Data Used in Model Development

Catalyst / Bed Parameters	
A_f, m^3/(mol.s)	25
E_a, J/mol	5x10^4
ABD, kg/m^3	900
ρ_{skel}, kg/m^3	3,900
ρ_{pe}, kg/m^3	1,900
Pellet porosity	0.592
Bed voidage	0.437
Total voidage	0.770
BET, m^2/g	54
Pore diam, nm	27

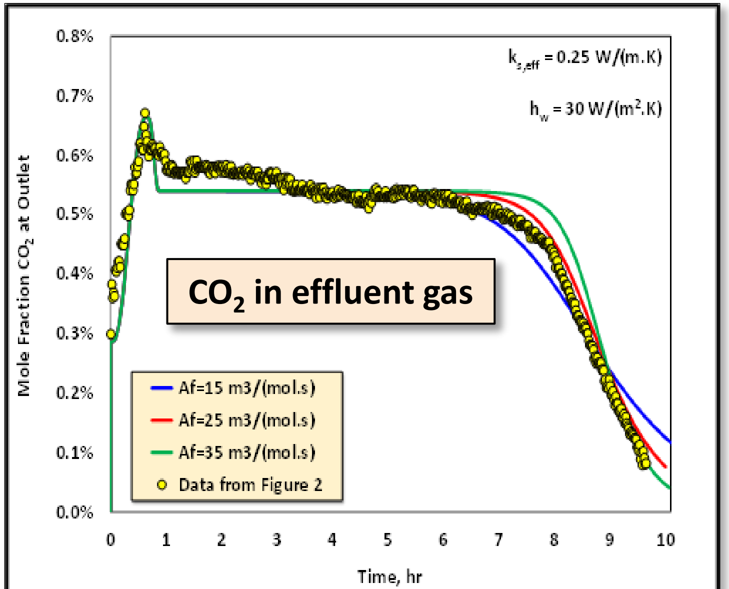

Thermal Parameters	
ΔH, J/mol	3.94x10^5
Thermal conductivity, W/(m.K)	$k_{s,eff}$
Wall heat transfer, W/(m^2.K)	h_w
Bulk heat capacity, J/(kg.K)	680

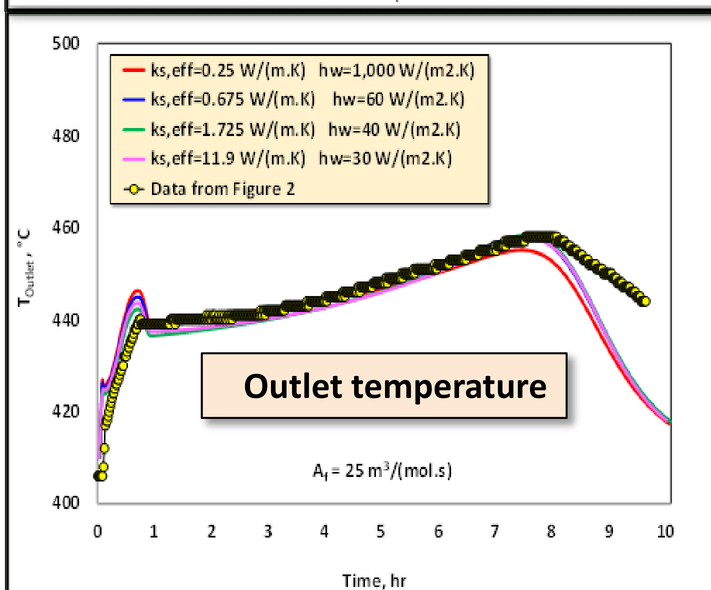

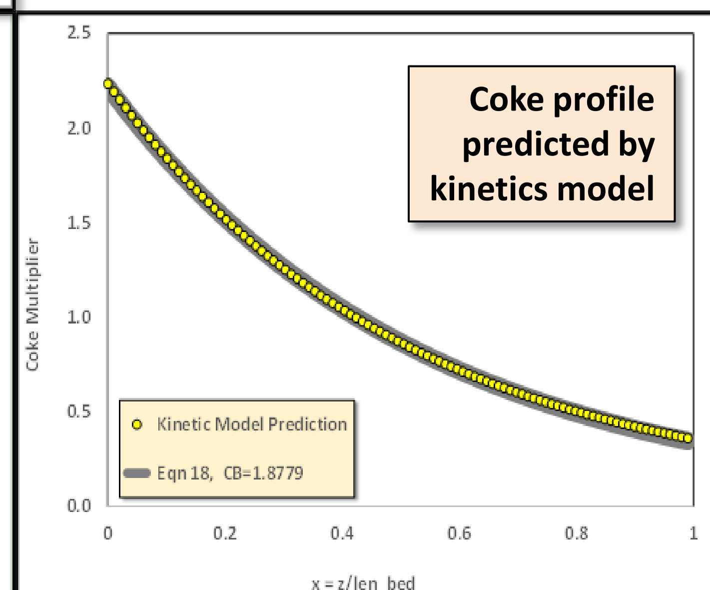

Biggest Unknown: Heat Transfer Parameters

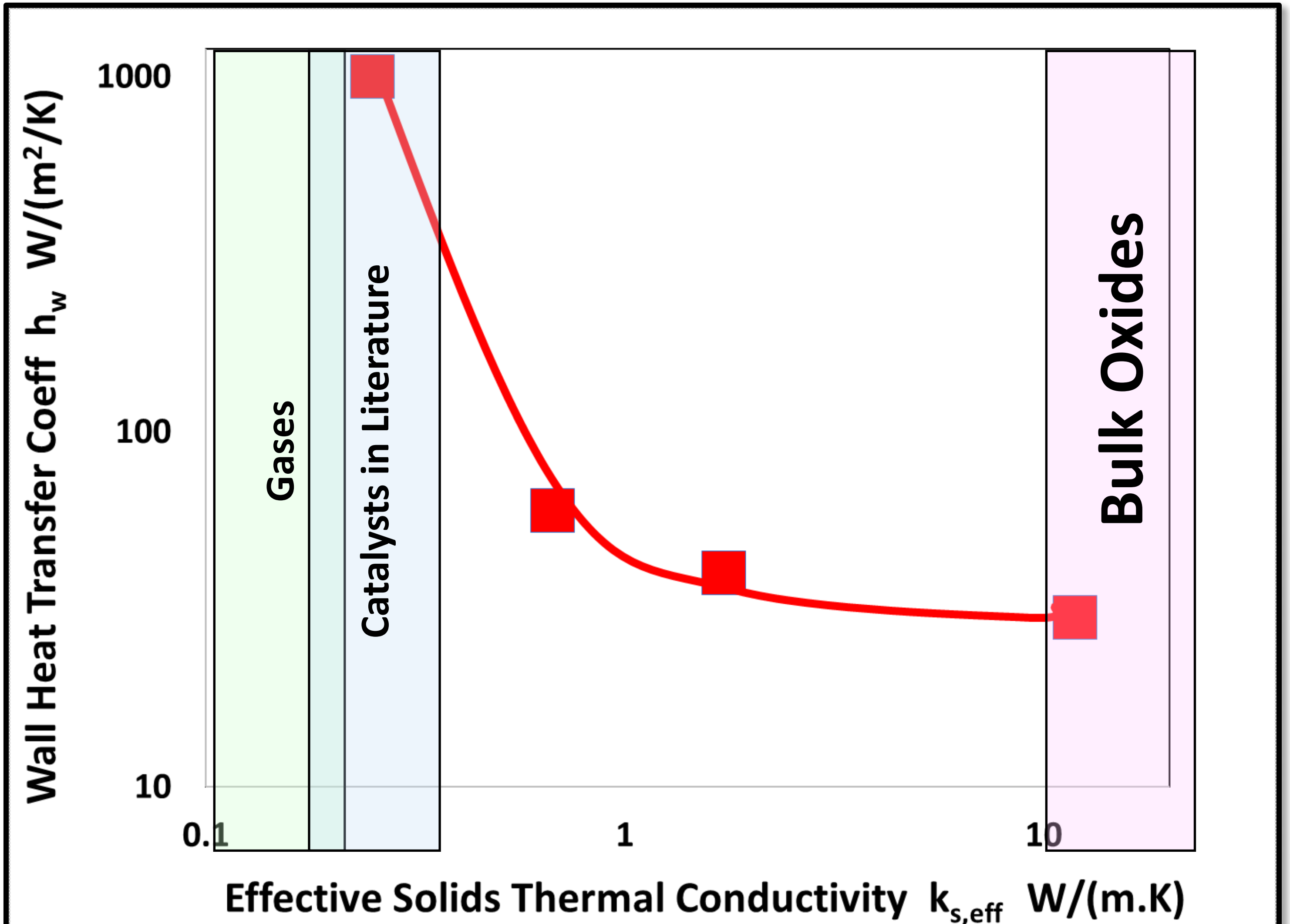

TCPDU Model Predictions

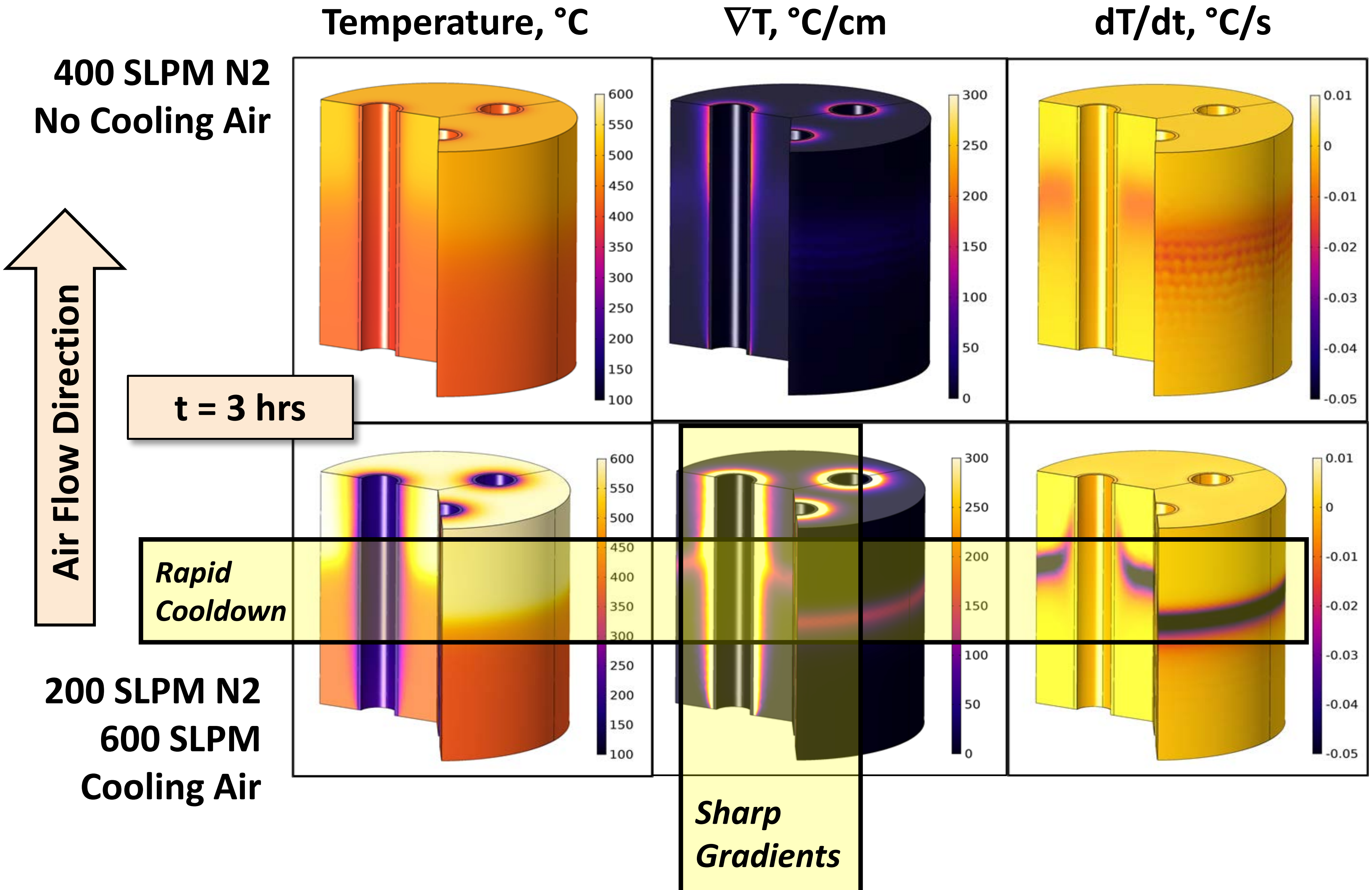

TCPDU Model Predictions (2)

200 SLPM N2, 600 SLPM Cooling Air

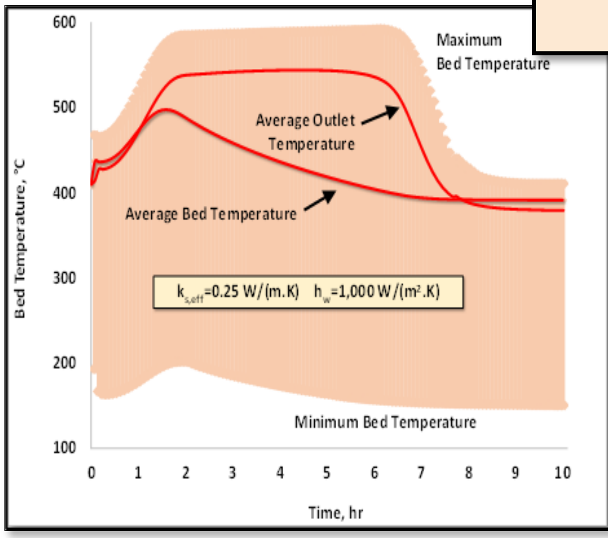

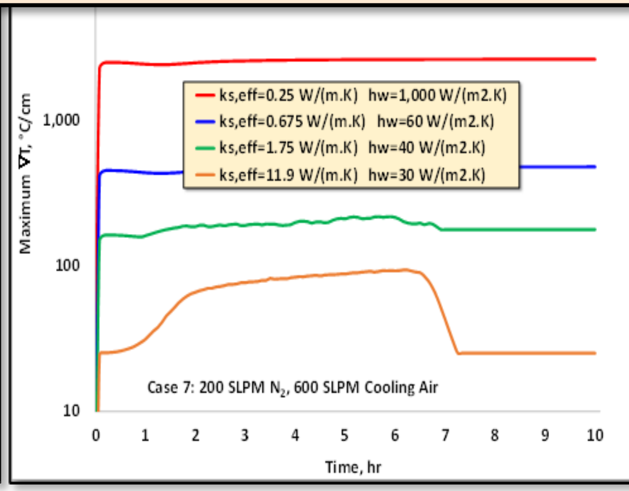

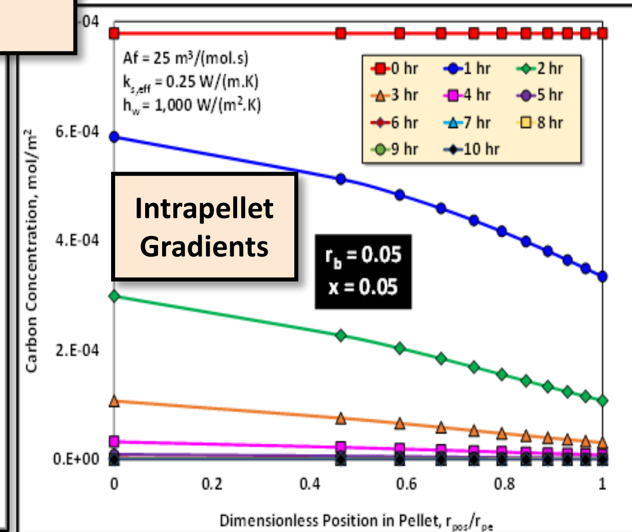

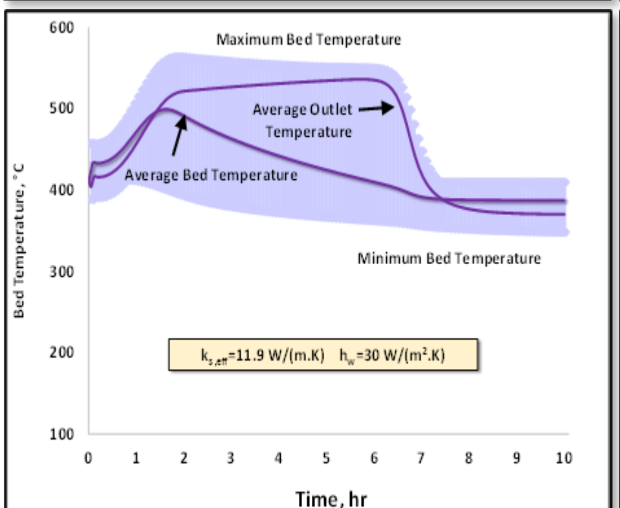

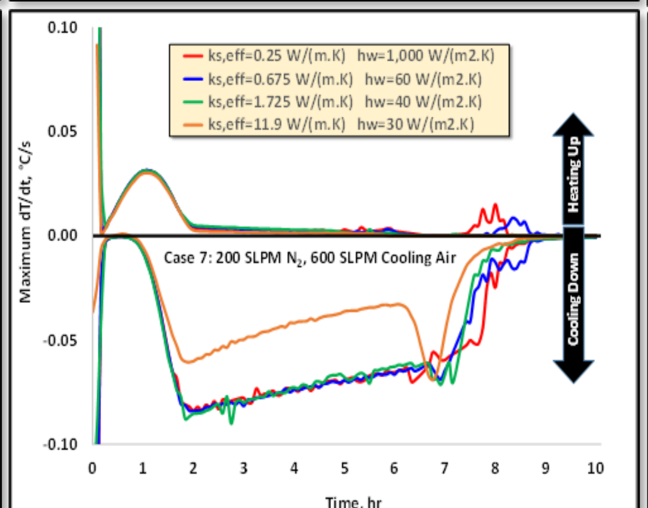

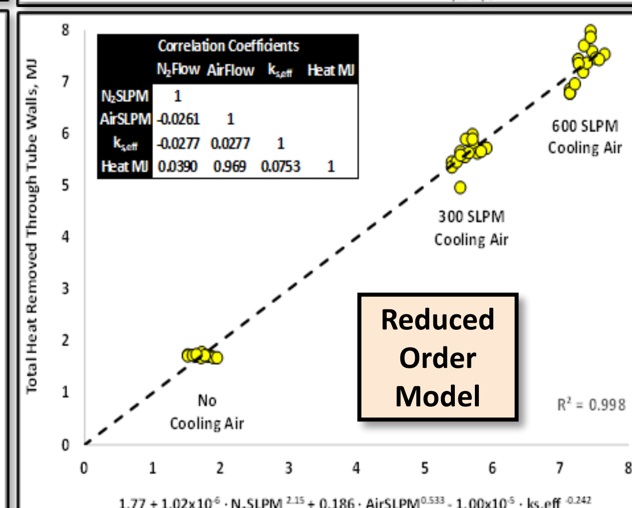

B.D. Adkins et.al, *Predicting thermal excursions during in-situ oxidative regeneration of packed bed catalytic fast pyrolysis catalyst,* submitted to *Reaction Chemistry and Engineering*

Conclusions

1. **Risk of catalyst damage and/or accelerated irreversible deactivation from thermal excursion is high in proposed TCPDU design**
   - **Pressure drop associated with small catalyst particle size (0.5 mm) constrains bed depth and process gas flow rate, both of which constrain heat removal**
2. **Potential design improvements**
   - **Construct reduced order models and throughly map catalyst / bed design space**
   - **Evaluate moving bed alternatives to packed bed. Not fluid bed: more like Continuous Catalytic Reformers (CCRs)**
3. **Although small by industry standards, a scale-up factor of 20 can be substantial, as demonstrated here**

Improvements in Reactor-Scale Models

1. **Firm up conclusions from regen model by addressing key unknowns**
   - **Thermal conductivity of catalyst pellets**
     - **Experimental measurements**
     - **High resolution mesoscale modelling of heat transfer**
   - **Coke distribution**
     - **Bed dissection**
     - **Carbon distribution in pellet interiors**
2. **Expand model to include stacked beds with multiple catalysts**

Stacked Bed Model

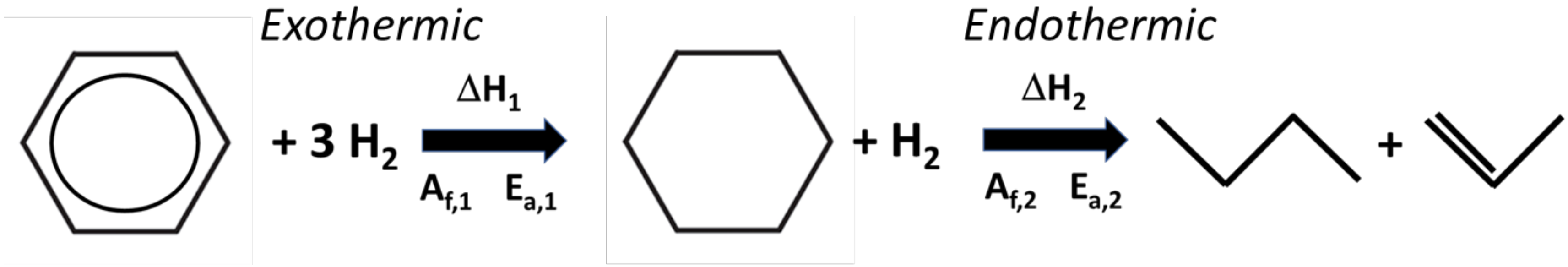

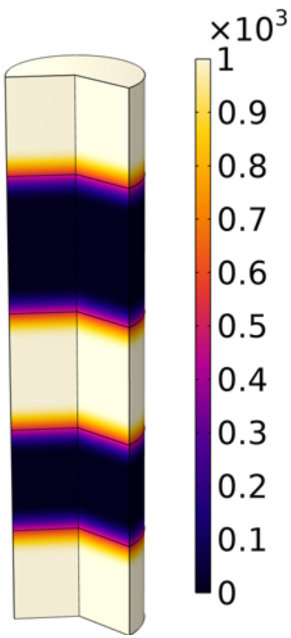

h_{wall}, W/(m².K)

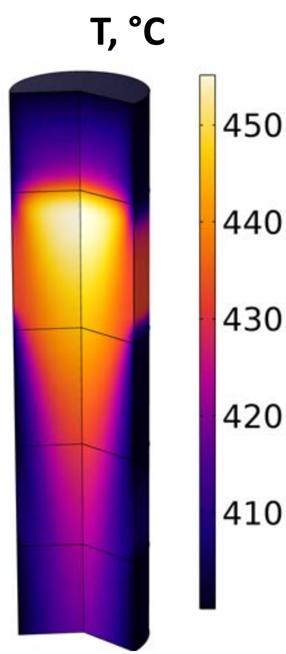

Bed-Specific Parameters
Mass of catalyst
ABD
Skeletal density
Particle size
Particle shape
Pore volume
Surface area
Pore diameter
Porosity
Void fraction
Thermal conductivity
Heat capacity
Wall heat transfer coeff.
Reaction rate constants
Reaction enthalpy
…

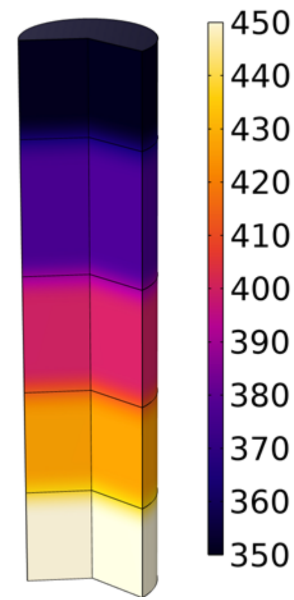

T_{wall}, °C

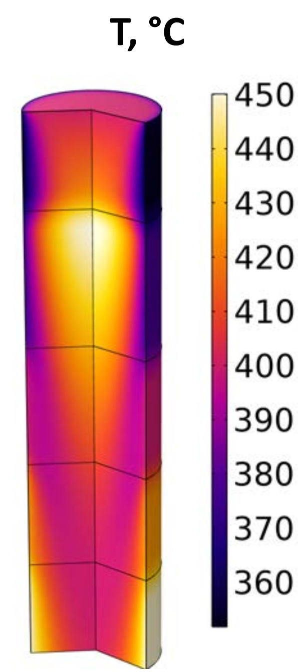

Stacked Bed Model

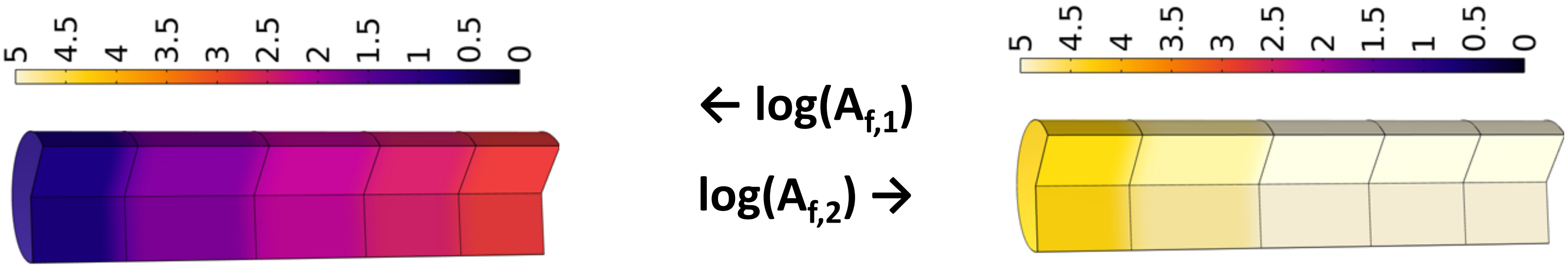

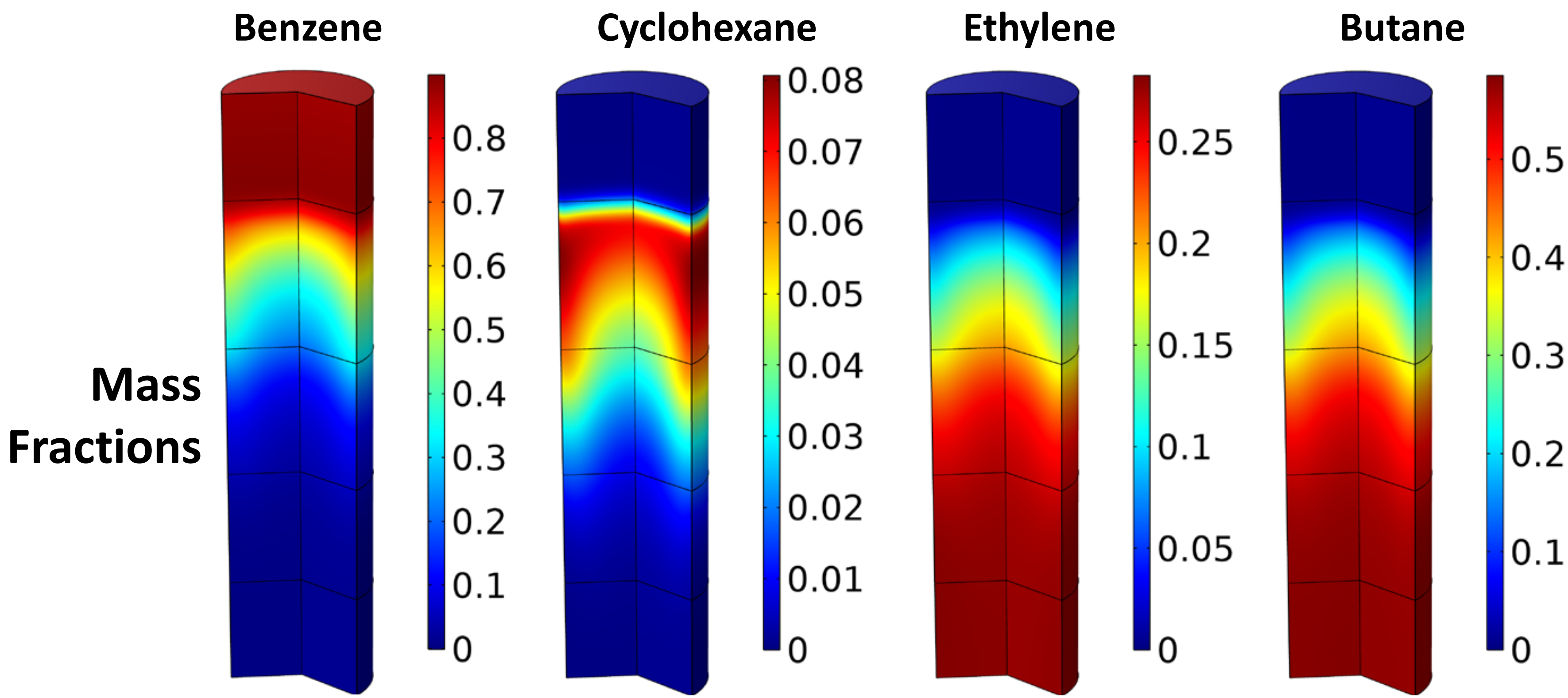

Acknowledgements

Fixed Bed CFP (NREL)
Joshua Schaidle
Calvin Mukarakate
Kristiina Iisa
Richard French
Kellene Orton
Scott Palmer
Fred Baddour
Dan Ruddy
Susan Habas
Connor Nash
Carrie Farberow
Matt Yung
Mark Nimlos
Anne Starace

Hydrotreating (PNNL)
Daniel (Miki) Santosa
Suh-Jane Lee
Igor Kutnyahov
Douglas C. Elliott
Huamin Wang

Packed Bed Modeling (NREL)
Vivek Bharadwaj
Meagan Crowley
Tom Foust
Aaron Lattanzi
Peter Ciesielski

Packed Bed Modeling (ORNL)
Zach Mills
Austin Ladshaw
James Parks II

TEA
Abhijit Dutta (NREL)
Kurt van Allsburg (NREL)
Sue Jones (PNNL)
Yunhua Zhu (PNNL)

Analysis (NREL)
Steve Deutch
Renee Happs
Anne Starace

Feedstock Logistics (INL)
Damon Hartley
Jordan Klinger

Fuel Properties (NREL)
Nolan Wilson
Earl Christensen
Lisa Fouts

NREL NATIONAL RENEWABLE ENERGY LABORATORY
OAK RIDGE National Laboratory
ChemCatBio Chemical Catalysis for Bioenergy
Energy Materials Network U.S. Department of Energy
INL Idaho National Laboratory
Pacific Northwest NATIONAL LABORATORY
U.S. DEPARTMENT OF ENERGY | Energy Efficiency & Renewable Energy
Bioenergy Technologies Office

Thank you. Let’s Discuss.

Michael.Griffin@nrel.gov

Brennan.Pecha@nrel.gov

Adkinsbd@ornl.gov

NREL/PR-5100-78854

Supporting Slides

ChemCatBio
Chemical Catalysis for Bioenergy

Vastly different operating conditions to match product yields

Description B:C, kg/kg	Pyrolysis only -	Pyrolysis only -	Base case 0.5% Pt 12	Test case 1% Pt 3	Test case 0.5% Pt 6	Test case 0.5% Pt 21
Feed	**CP/FR**	**CP**	**CP/FR**	**CP**	**CP/FR**	**CP/FR**
# of runs	3	3	4	3	1	1
Organics in Oil	58.5±0.5	56.3±0.1	24.7±0.1	20.9±0.1	23	26.6
Organics in Aqueous Phase	0.0±0.0	0.0±0.0	3.8±0.3	2.3±0.0	3.5	4.0
Water	13.3±0.2	17.5±0.4	21.7±0.0	22.9±0.3	21.9	20.1
Light Condensables	2.3±0.1	0.5±0.2	10.0±0.2	8.0±0.1	8.6	9.9
Light gases	15.2±0.3	13.9±0.8	28.2±0.5	31.6±0.3	29.2	27.4
CH_4	*1.3±0.0*	*0.5±0.1*	*3.2±0.1*	*3.2±0.0*	*3.2*	*3.0*
CO	*7.5±0.2*	*6.1±0.4*	*14.5±0.6*	*15.7±0.2*	*15.0*	*14.6*
CO_2	*5.6±0.1*	*6.0±0.3*	*7.6±0.1*	*8.1±0.1*	*8.0*	*7.3*
C_2-C_4	*0.9±0.0*	*0.7±0.0*	*2.8±0.1*	*4.0±0.0*	*3.0*	*2.5*
Char	10.7±0.0	11.8±0.6	10.3±0.0	11.8±0.3	12.3	10.9
Coke	-	-	1.4±0.0	2.5±0.1	1.8	1.1

Vastly different operating conditions to match oil quality

	Run	Pyrolysis only	0.5% Pt	1% Pt	0.5% Pt	0.5% Pt
	B:C, kg/kg	-	12	3	6	21
Description	Feed	CP	CP/FR	CP	CP/FR	CP/FR
HC	Aromatic hydrocarbons	0.02	1.3±0.2	2.8±0.8	1.6	0.8
HC	Alkanes+Alkenes	0.02	0.5±0.1	0.6±0.3	1.0	1.3
OX	Cyclopente/anones	0.99	8.0±0.2	9.2±0.5	7.8	8.3
PV	Other Ketones/aldehydes	4.15	5.4±0.1	4.2±0.1	6.6	3.4
OX	Phenol	0.19	4.6±0.2	7.0±0.7	5.2	4.6
OX	Methylphenols	0.18	1.7±0.1	2.9±0.2	2.0	1.6
OX	Other phenols	0.36	6.1±0.6	11.5±2.2	7.4	6.2
OX	Furanics	2.29	4.1±0.1	1.9±0.1	2.6	7.2
PV	Acids	1.42	0.9±0.1	1.3±0.3	1.3	2.6
PV	Methoxyphenols	0.92	0.6±0.1	1.2±0.4	0.4	1.7
PV	Sugars	0.57	0.0±0.0	0.0±0.0	0.0	0.2
PV	Other oxygenates	2.54	1.4±0.2	1.9±0.4	0.7	1.9
	Total, wt% in oil	13.66	34.7	44.4	36.5	39.8

Apparent rate constants fit to real data

Model initial values and boundary conditions

Parameter	Value	Description
L	0.14 m	length of reactor bed
P_{tot}	1E5 Pa	pressure in reactor, inlet
u_{inf}	0.947 m/s	nominal gas velocity
U	2.167 m/s	void fraction-corrected gas velocity
T_{in}	450 C	temperature reactor
ρ_g	0.2247 kg/m^3	density gas ([85% H_2 + 15% N_2] + PV + LG + H2O), inlet
μ_{vap}	1.97E-5 kg/m.s	estimated viscosity of gas + PV
AFR	7.5E-4 m^3/s	actual volumetric flowrate gas
$mfPVin_{50/50\ CP/FR}$	0.458	mass fraction LMW PV in for 50/50 CP/FR
$mfPVin_{CP}$	0.417	mass fraction LMW PV in for CP
D_i	4E-5 m^2/s	bulk diffusion coefficient for all species
$D_{i,eff}$	$D_i\ \varepsilon_{ps}$	effective bulk diffusion coefficient
ε_{ps}	0.437	void fraction reactor bed
ε_{pp}	0.592	void fraction catalyst particle
D_p	0.5E-3 m	diameter catalyst particle
D_{pore}	2.8E-8 m	pore diameter of catalyst particles
Re	12.4	Reynolds number with respect to particle
T	7 $48.5 D_{pore}\sqrt{T/MW}$	tortuosity within catalyst particle
K_D		Knudsen diffusion coefficient calculation
Re	28	Reynolds number with respect to a single catalyst particle with inlet fluid properties
Sc	5	Schmidt number
Pe	141	Peclet number
Sh	152	Sherwood number for creeping flow around sphere[36]

Lumped rate constants fit with Matlab for base case

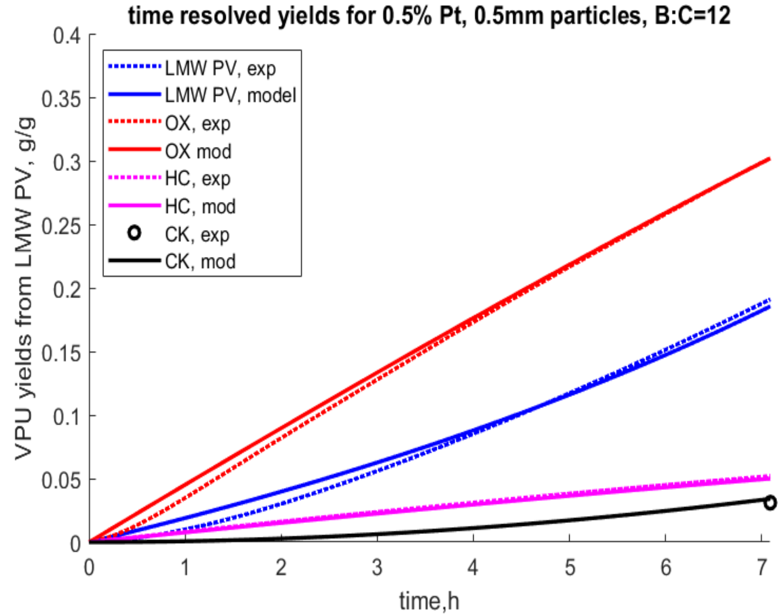

RATE CONSTANT	FITTED VALUE
k1 [s^{-1}]	76
k1g [s^{-1}]	50.5
k1w [s^{-1}]	39
k2 [s^{-1}]	5.4
k2g [s^{-1}]	0.7
k2w [s^{-1}]	7.9E-10
k3 [s^{-1}]	7E-14
k4 [s^{-1}]	3.7E-4
Θ_{S1}	1.2E-3
Θ_{S2}	15.2